

Supporting material

Modification of Thermally Activated Delayed Fluorescence Emitters Comprising Acridan- pyrimidine Moieties for Efficient Sky-Blue to Greenish-Blue OLEDs

Yi-Zhen Li^a, Hsuan-Chi Liang^a, Chia-Hsun Chen^b, Ching-Huang Chiu^b,
Bo-Yen Lin^{c*}, Jake A. Tan^{d*}, Jiun-Haw Lee^{b*}, Tien-Lung Chiu^{e*} and Man-kit
Leung^{a,f*}

^a Department of Chemistry, National Taiwan University, Taipei 10617, Taiwan.

^b Graduate Institute of Photonics and Optoelectronics and Department of Electrical Engineering,
National Taiwan University, Taipei 10617, Taiwan.

^c Department of Opto-Electronic Engineering, National Dong Hwa University,
Shoufeng, Hualien 974301, Taiwan.

^d Department of Chemistry, Gottwald Center for the Sciences, University of Richmond,
Richmond, Virginia 23173, USA

^e Department of Electrical Engineering, Yuan Ze University, Chung-Li, Taoyuan 32003, Taiwan.

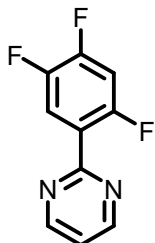
^f Advanced Research Center for Green Materials Science and Technology, National Taiwan
University No. 1, Sec. 4, Roosevelt Rd., Taipei 10617, Taiwan (R.O.C.)

Email:boyenlin@gms.ndhu.edu.tw ; jiunhawlee@ntu.edu.tw; mkleung@ntu.edu.tw;

tlchiu@saturn.yzu.edu.tw; jake.tan@richmond.edu

Experimental Section

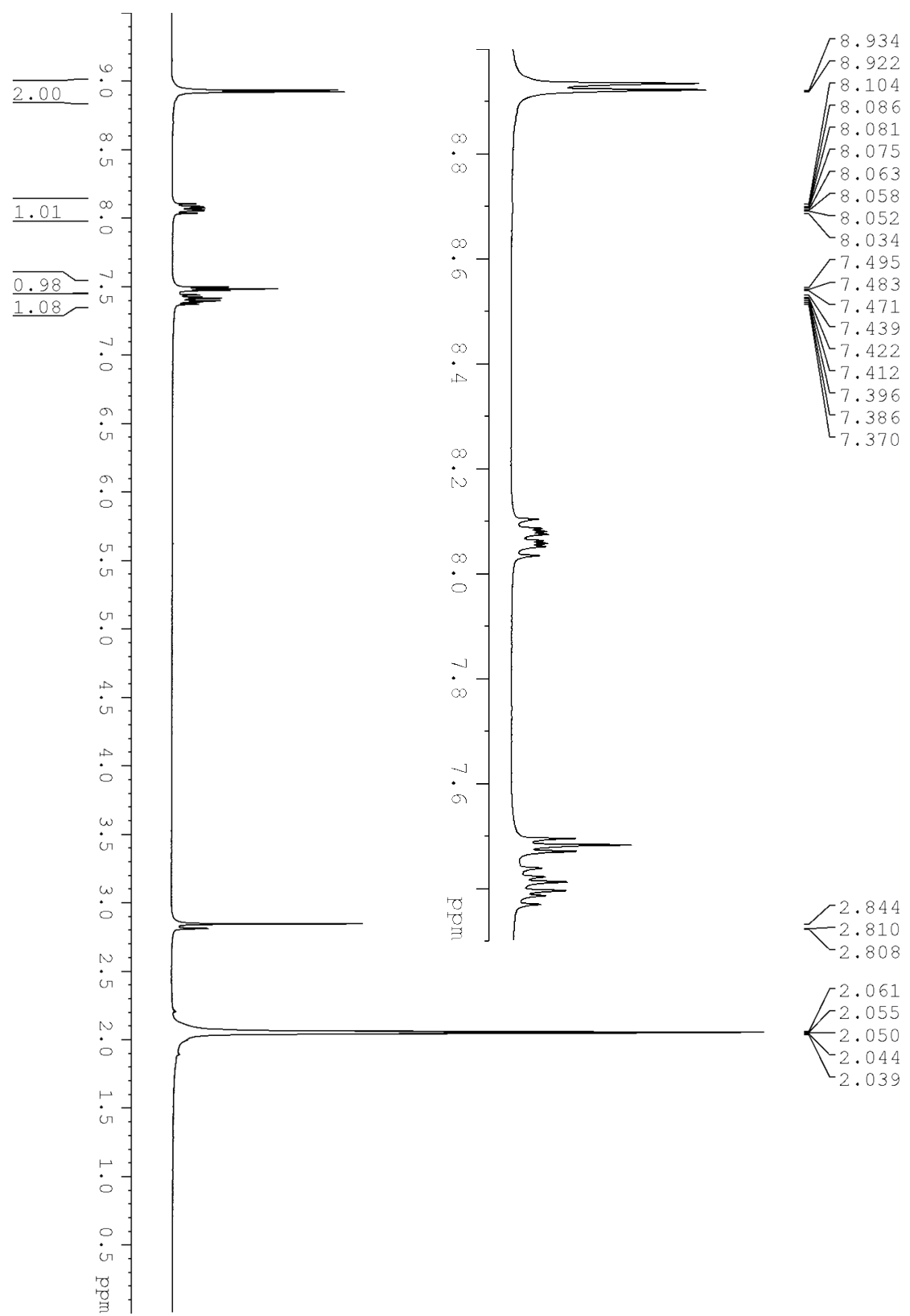
2-(2,4,5-trifluorophenyl)pyrimidine (**1**)



A mixture of 2,4,5-trifluorophenylboronic acid (5.842 g, 33.21 mmol), 2-bromopyrimidine (3.5 g, 22.14 mmol), Pd(OAc)₂ (0.2485 g, 1.107 mmol) and triphenylphosphine (1.155 g, 4.428 mmol) were flushed with argon then methoxymethane (22 mL) and potassium carbonate solution (21 mL, 2.7 M, 56.7 mmol) were added respectively. The resulting mixture was refluxed at 105°C for 2.5 hours. After the reaction, the solvent was removed by vacuum distillation. The residue was extracted with dichloromethane and water. The organic layer was dried over anhydrous MgSO₄ and removed under reduced pressure. The crude product was purified through column chromatography with dichloromethane and afford compound **1** as a white solid (3.2970 g, 70 % yield).

¹H NMR (400 MHz, Acetone-*d*₆): δ 8.93 (d, *J* = 4.8 Hz, 2 H), δ 8.10-8.03 (m, 1 H), δ 7.48 (t, *J* = 4.8 Hz, 1 H), δ 7.44-7.37 (m, 1 H); ¹³C NMR (100 MHz, Chloroform-*d*₁): δ 161.73 (d, ³*J*_{CF} = 6 Hz), 157.35, 156.70 (ddd, ¹*J*_{CF} = 254 Hz, ²*J*_{CF} = 9 Hz, ³*J*_{CF} = 2 Hz), 151.37 (ddd, ¹*J*_{CF} = 254 Hz, ²*J*_{CF} = 15 Hz, ³*J*_{CF} = 12 Hz), 146.80 (ddd, ¹*J*_{CF} = 244 Hz, ²*J*_{CF} = 13 Hz, ³*J*_{CF} = 4 Hz), 122.7, 119.70 (d, ²*J*_{CF} = 21 Hz), 107.02 (d, ²*J*_{CF} = 21 Hz), 106.87 (d, ²*J*_{CF} = 21 Hz); HRMS calcd. for C₁₀H₆F₃N₂ (M+1⁺) 211.0478, obsd. 211.0486

Figure S1. ^1H NMR spectrum of compound (**1**).



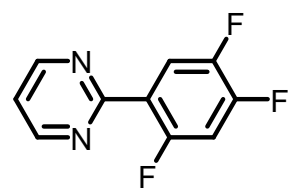


Figure S2. ^{13}C NMR spectrum of compound (**1**).

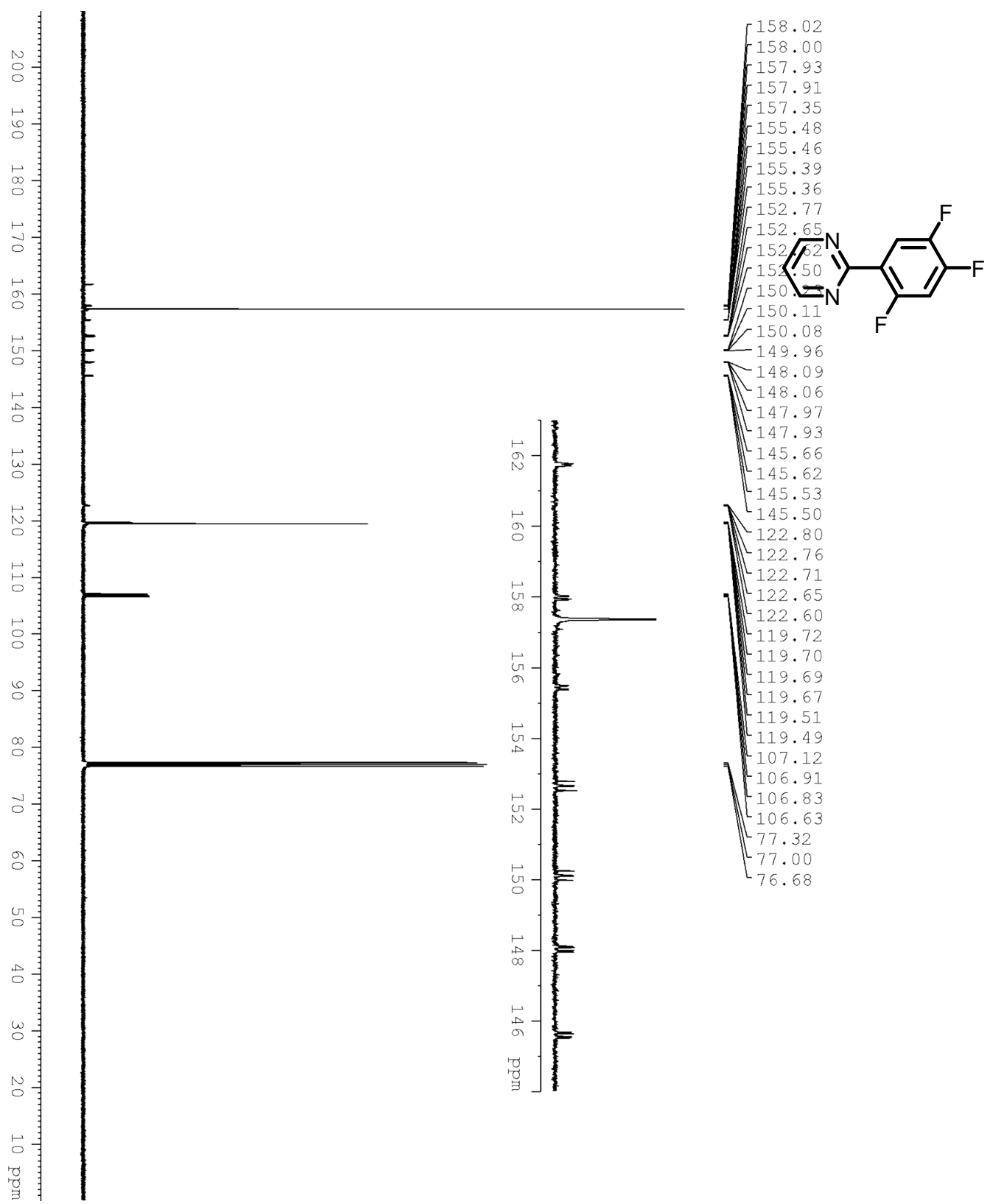
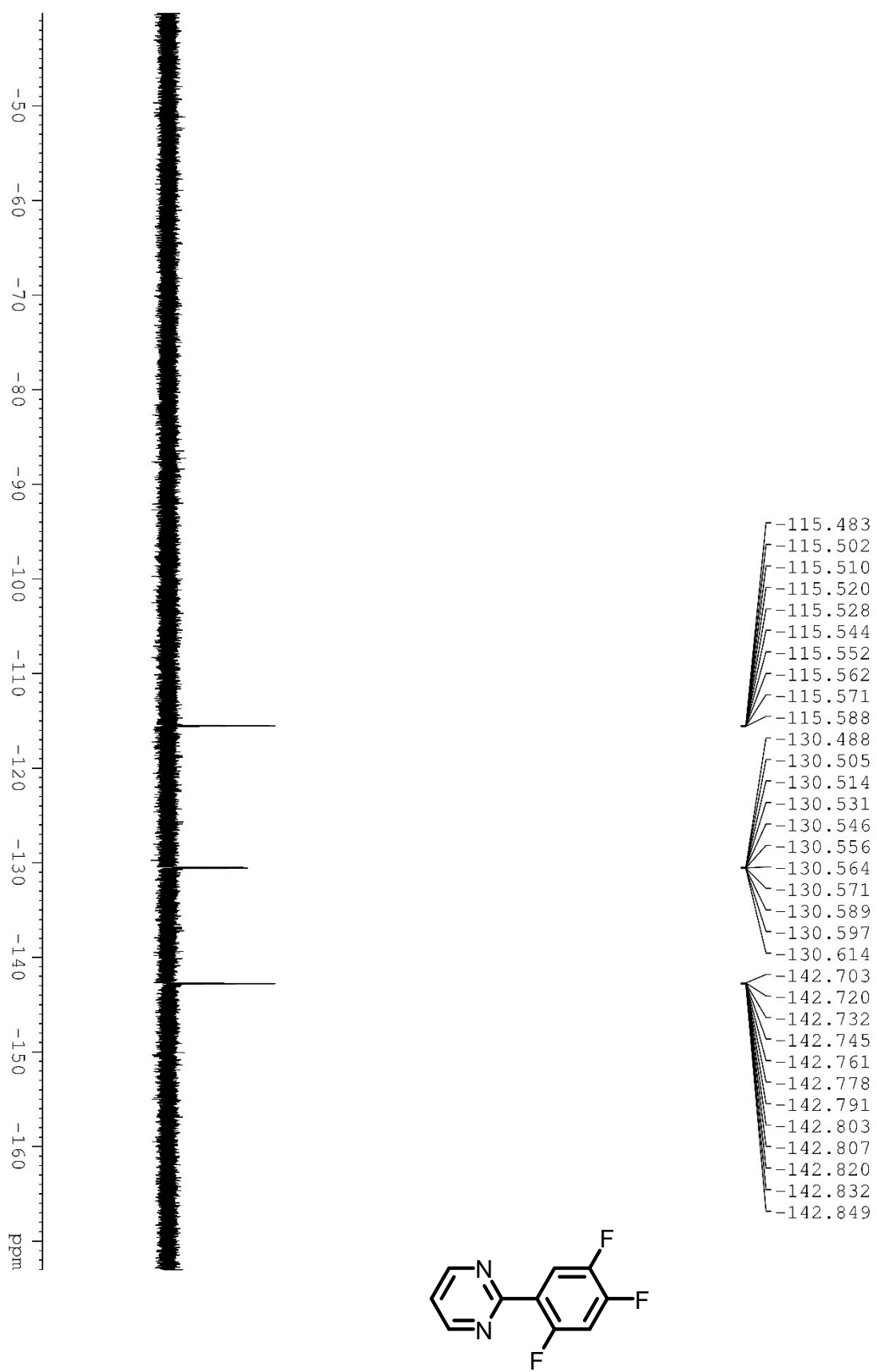
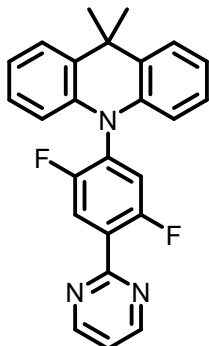


Figure S3. ^{19}F NMR spectrum of compound (**1**).



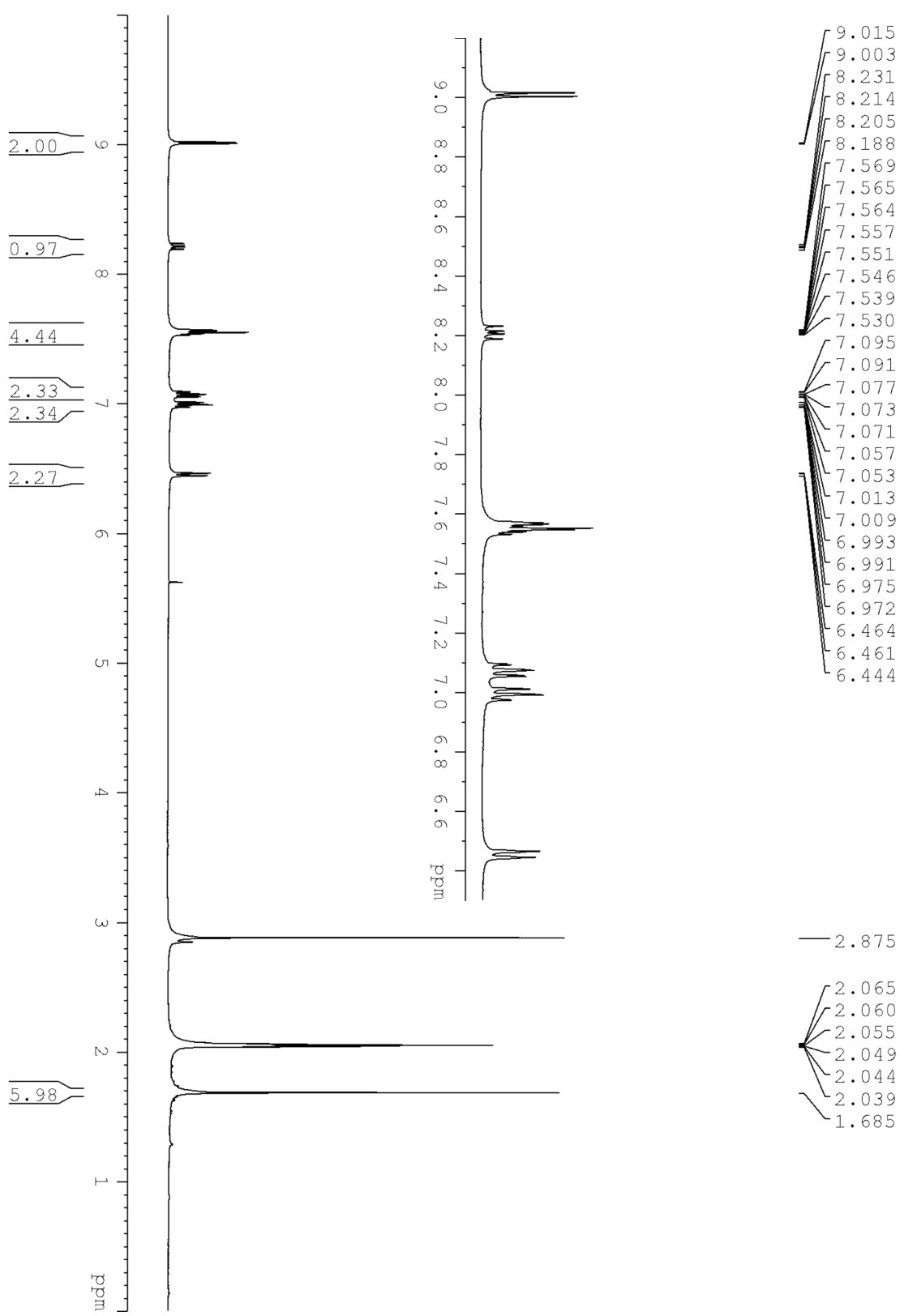
10-(2,5-difluoro-4-(pyrimidin-2-yl)phenyl)-9,9-dimethyl-9,10-dihydroacridine (3)



A mixture of **1** (0.8 g, 3.807 mmol), 9,9-dimethyl-9,10-dihydroacridine (0.956 g, 4.568 mmol) and Cs_2CO_3 (2.480 g, 7.614 mmol) were dissolved in dimethyl sulfoxide (3.8 mL) under argon atmosphere. The mixture was stirred at 120°C for 16 hours. After the reaction, the solvent was removed by vacuum distillation. The residue was extracted with dichloromethane and water. The organic layer was dried over anhydrous MgSO_4 and removed under reduced pressure. The crude product was purified through column chromatography with dichloromethane and afford compound **3** as a white solid (0.524 g, 35 % yield).

^1H NMR (400 MHz, Acetone- d_6): δ 9.01 (d, $J = 4.8$ Hz, 2 H), δ 8.21 (dd, $J = 10.4, 6.8$ Hz, 1 H), δ 7.57-7.53 (m, 4 H), δ 7.07 (td, $J = 7.2, 1.6$ Hz, 2 H), δ 6.99 (td, $J = 7.2, 1.6$ Hz, 2 H), δ 6.45 (d, $J = 6.8$ Hz, 2 H), 1.69 (s, 6 H); ^{13}C NMR (100 MHz, Acetone- d_6): δ 162.58 (dd, $^2J_{CF} = 6$ Hz, $^3J_{CF} = 2$ Hz), 159.46 (dd, $^1J_{CF} = 142$ Hz, $^2J_{CF} = 2$ Hz), 158.67, 156.96 (dd, $^1J_{CF} = 133$ Hz, $^2J_{CF} = 3$ Hz), 140.53, 131.58 (dd, $^1J = 17$ Hz, $^2J = 10$ Hz), 131.43, 129.56 (dd, $^1J = 12$ Hz, $^2J = 8$ Hz), 127.76, 126.36, 122.64 (dd, $^1J = 25$ Hz, $^2J = 2$ Hz), 122.48, 121.33, 120.83 (dd, $^1J = 24$ Hz, $^2J = 3$ Hz), 114.28, 36.77, 31.32; HRMS calcd. for $\text{C}_{25}\text{H}_{20}\text{F}_2\text{N}_3$ ($\text{M}+1^+$) 400.1620, obsd. 400.1626

Figure S4. ^1H NMR spectrum of compound (3).



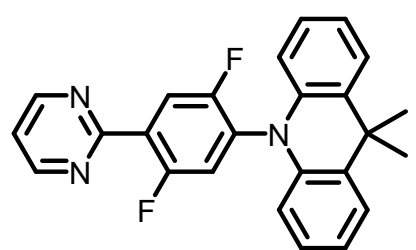


Figure S5. ^{13}C NMR spectrum of compound (3).

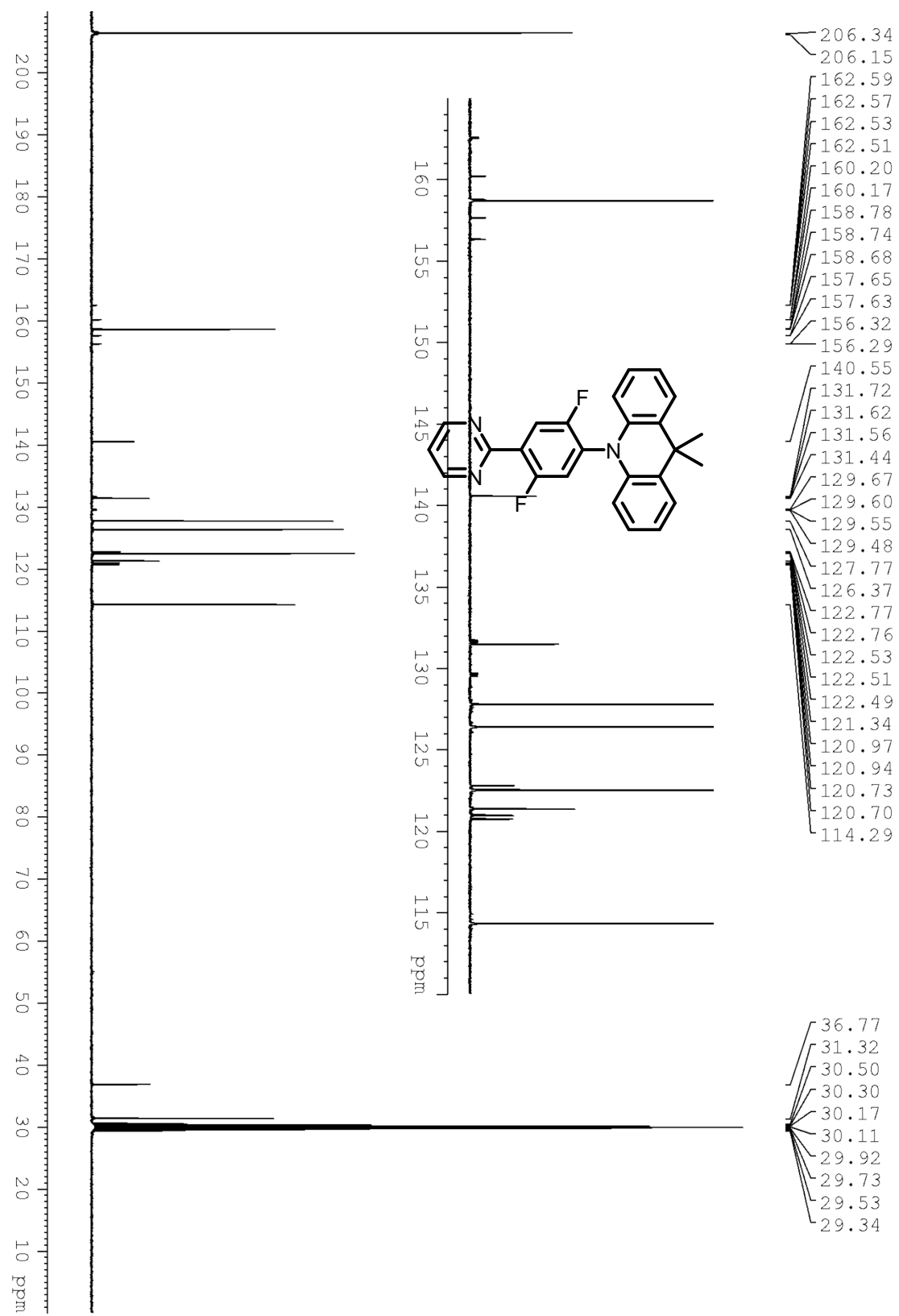
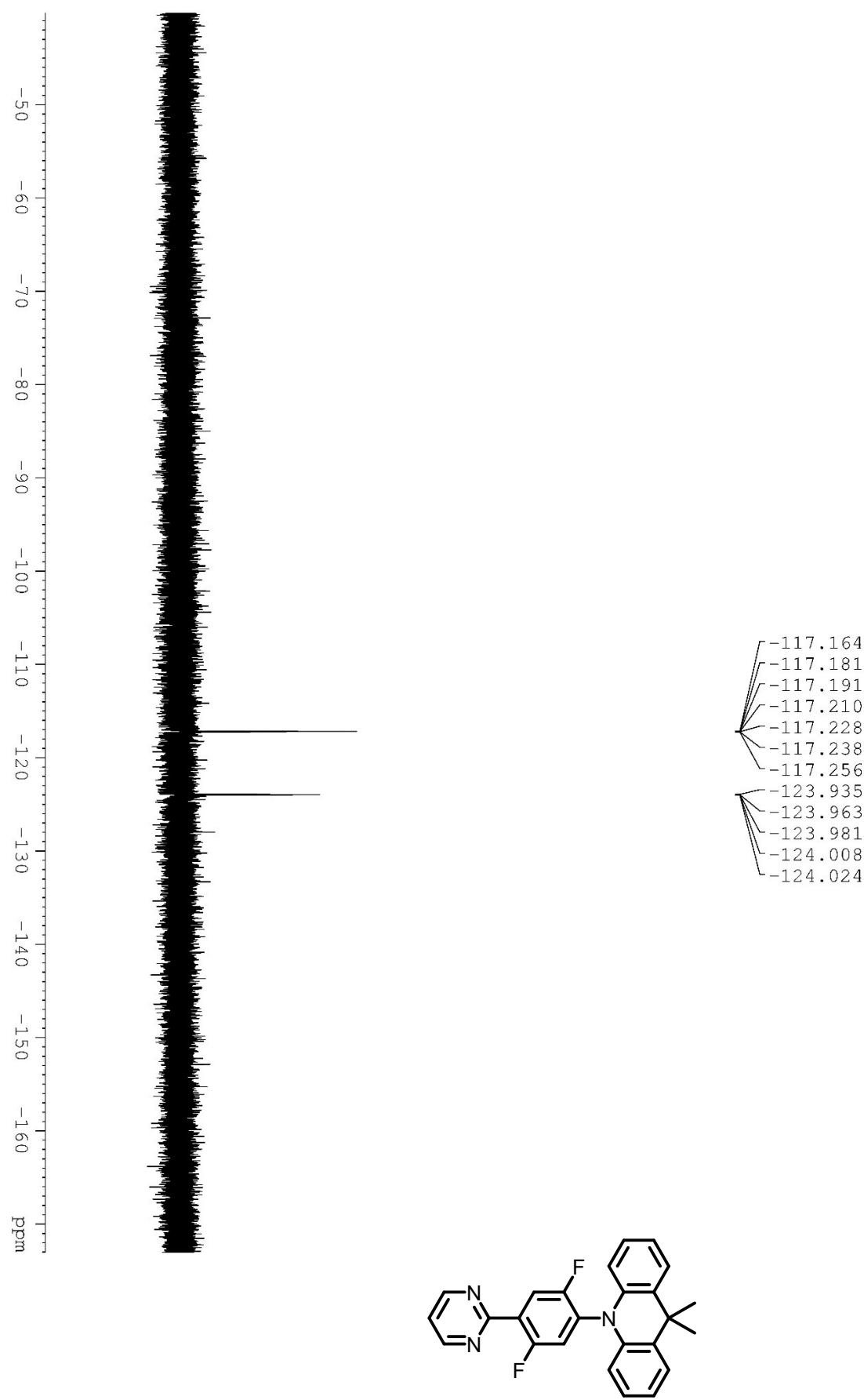
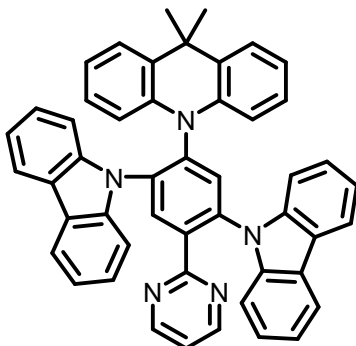


Figure S6. ^{19}F NMR spectrum of compound (3).



10-(2,5-di(9H-carbazol-9-yl)-4-(pyrimidin-2-yl)phenyl)-9,9-dimethyl-9,10-dihydroacridine (4Ac25CzPy)



A mixture of **3** (1.534 g, 3.8 mmol), carbazole (2.565 g, 15.34 mmol) and Cs_2CO_3 (3.714 g, 11.4 mmol) was dissolved in dimethyl sulfoxide (3.8 mL) under argon atmosphere and stirred at 120°C for 16 hours. After the reaction, the solvent was removed by vacuum distillation. The residue was extracted with dichloromethane and water. The organic layer was dried over anhydrous MgSO_4 and removed under reduced pressure. The crude product was purified through column chromatography with 1:1 v/v mixture of hexane and dichloromethane. The product was heat flushed in acetone and afford **4Ac25CzPy** as a yellow solid (2.0 g, 76 % yield).

^1H NMR (400 MHz, Methylene Chloride- d_2): δ 8.65 (s, 1 H), δ 8.38 (d, $J = 4.8$ Hz, 2 H), δ 8.12 (d, $J = 8$ Hz, 2 H), δ 8.12 (s, 1 H), δ 7.98-7.96 (m, 2 H), δ 7.43 (d, $J = 8$ Hz, 2 H), δ 7.35 (t, $J = 8$ Hz, 2 H), δ 7.27-7.21 (m, 6 H), 7.17-7.11 (m, 4 H), 7.06 (t, $J = 8$ Hz, 2 H), 6.94-6.91 (m, 3 H), δ 6.87 (t, $J = 7.4$ Hz, 2 H), 1.62 (s, 3 H), 0.06 (s, 3 H);
 ^{13}C NMR (100 MHz, Methylene Chloride- d_2): δ 164.35, 157.60, 142.09, 141.65, 141.37, 140.58, 138.90, 137.88, 136.78, 135.98, 131.32, 126.69, 126.53, 125.97, 125.27, 124.18, 123.82, 121.84, 120.77, 120.55, 120.40, 120.38, 119.80, 114.26, 110.99, 110.08, 36.07; HRMS calcd. for $\text{C}_{49}\text{H}_{36}\text{N}_5$ ($\text{M}+1^+$) 694.2965, obsd. 694.2959; Elemental analysis calcd. for C (84.82%), N (10.09%), H (5.08%), obsd. C (84.630%), N (10.090%), H (4.949%)

Figure S7. ^1H NMR spectrum of 4Ac25CzPy.

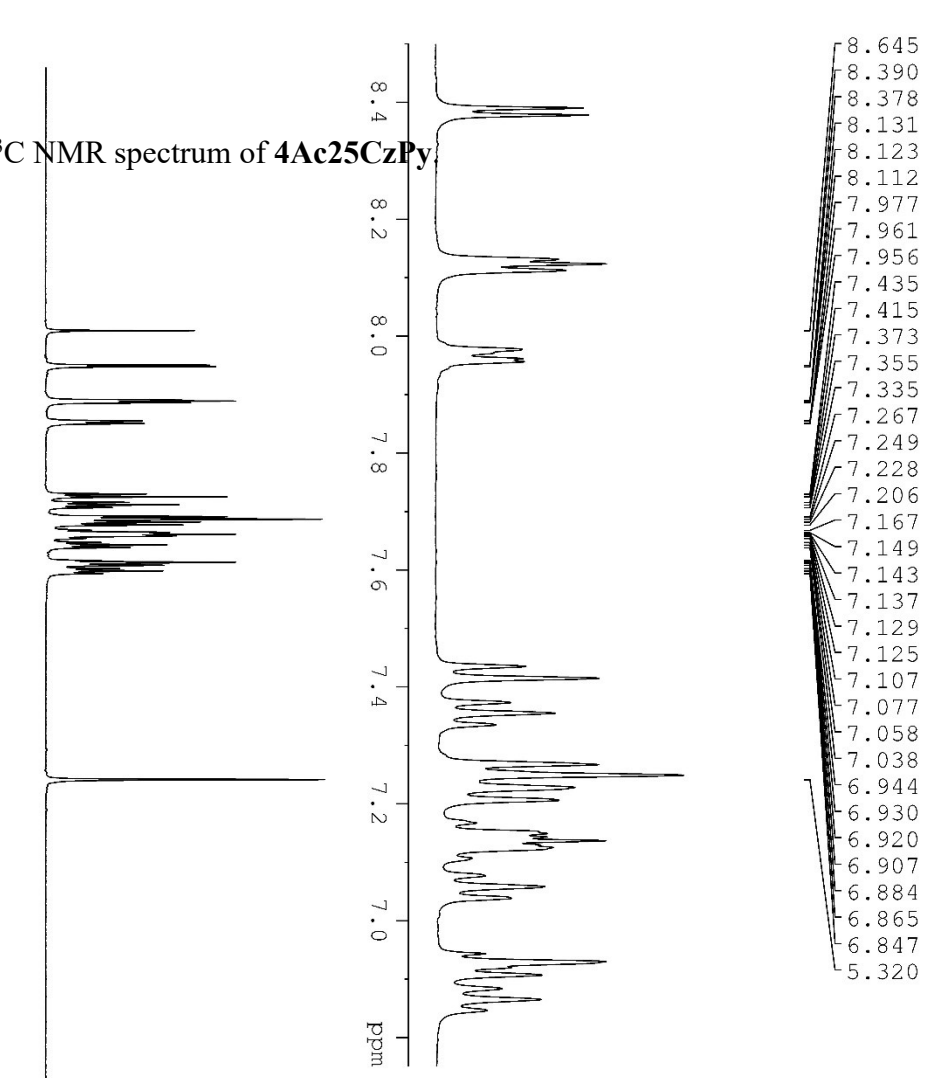
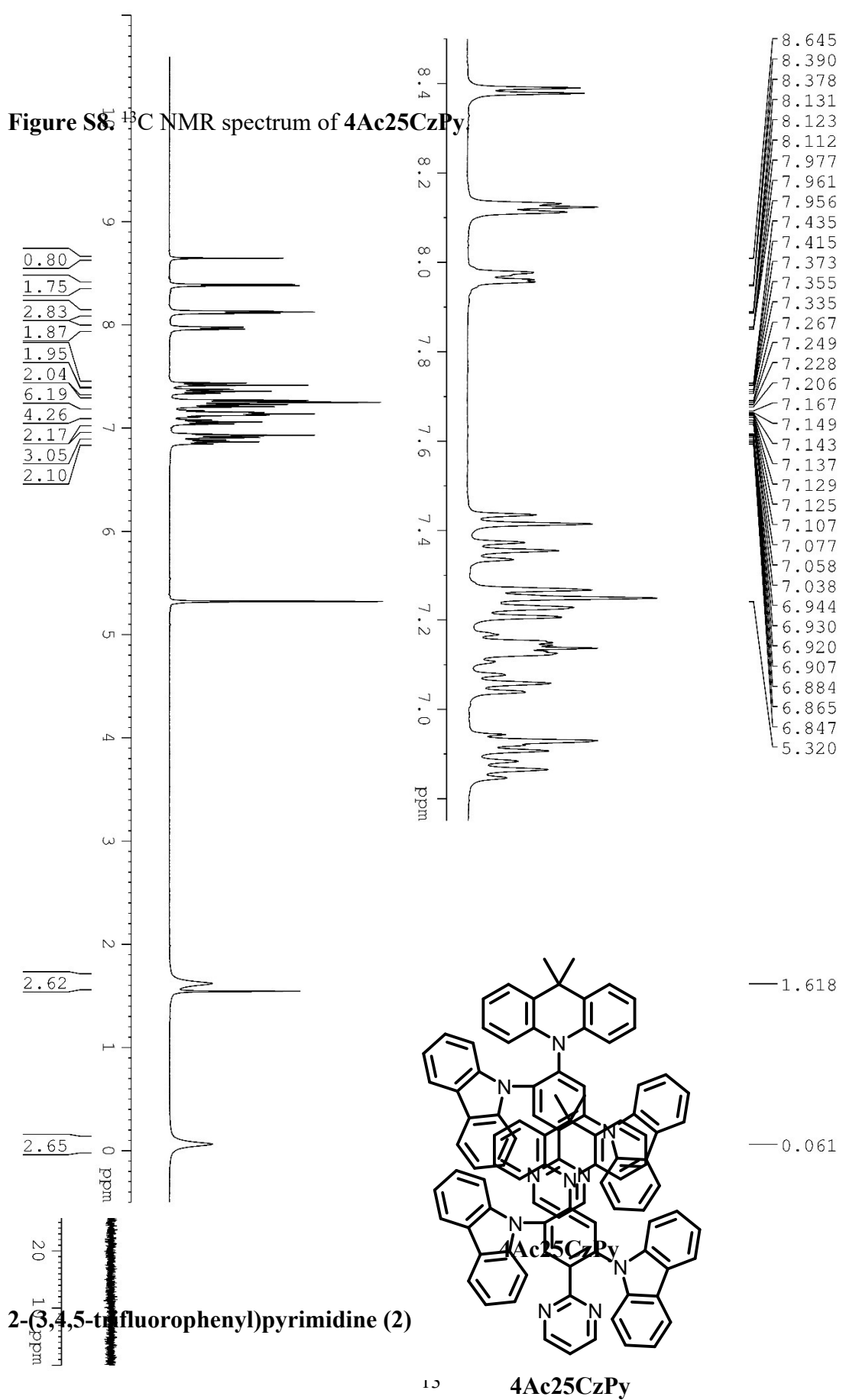
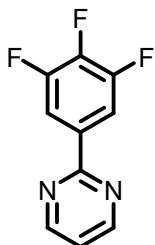


Figure S8. ^{13}C NMR spectrum of 4Ac25CzPy





A mixture of 3,4,5-trifluorophenylboronic acid (4.299 g, 30 mmol), 2-bromopyrimidine (1.592 g, 10 mmol), K₂CO₃ (5.526 g, 40 mmol) and Pd(PPh₃)₄ (0.4622 g, 0.4 mmol,) were dissolved in 1,4-dioxane (16 mL) and H₂O (4 mL) under argon atmosphere . The mixture was stirred at 90 °C for 3 hours. After the reaction, the solvent was removed by vacuum distillation. The residue was dissolved in DCM and washed with water and K₂CO_{3(aq)}. The organic layer was dried by anhydrous MgSO₄. The crude was purified through chromatography with Hexanes/ EA = 4/1 as eluent to afford purified product **2** as a white solid (1.281 g, 61 % yield).

¹H NMR (400 MHz, Acetone-*d*₆): δ 8.89 (d, *J* = 4.8 Hz, 2 H), δ 8.14 (dd, *J*₁ = 9.2 Hz, *J*₂ = 7.2 Hz, 2 H), δ 7.47 (t, *J* = 4.8 Hz, 1 H), ¹³C NMR (100 MHz, Acetone-*d*₆): δ 161.90, 158.71, 152.114 (ddd, ¹*J*_{CF} = 248 Hz, ²*J*_{CF} = 10 Hz, ³*J*_{CF} = 3.5 Hz), 142.17 (dt, ¹*J*_{CF} = 254 Hz, ²*J*_{CF} = 16 Hz), 135.41 (td, ²*J*_{CF} = 8.0 Hz, ³*J*_{CF} = 4.0 Hz), 121.46, 112.92 (dd, ²*J*_{CF} = 17 Hz, ³*J*_{CF} = 7 Hz); HRMS calcd. for C₁₀H₆F₃N₂ (M+1⁺) 211.0478, obsd. 211.0483

Figure S9. ^1H NMR spectrum of compound (2).

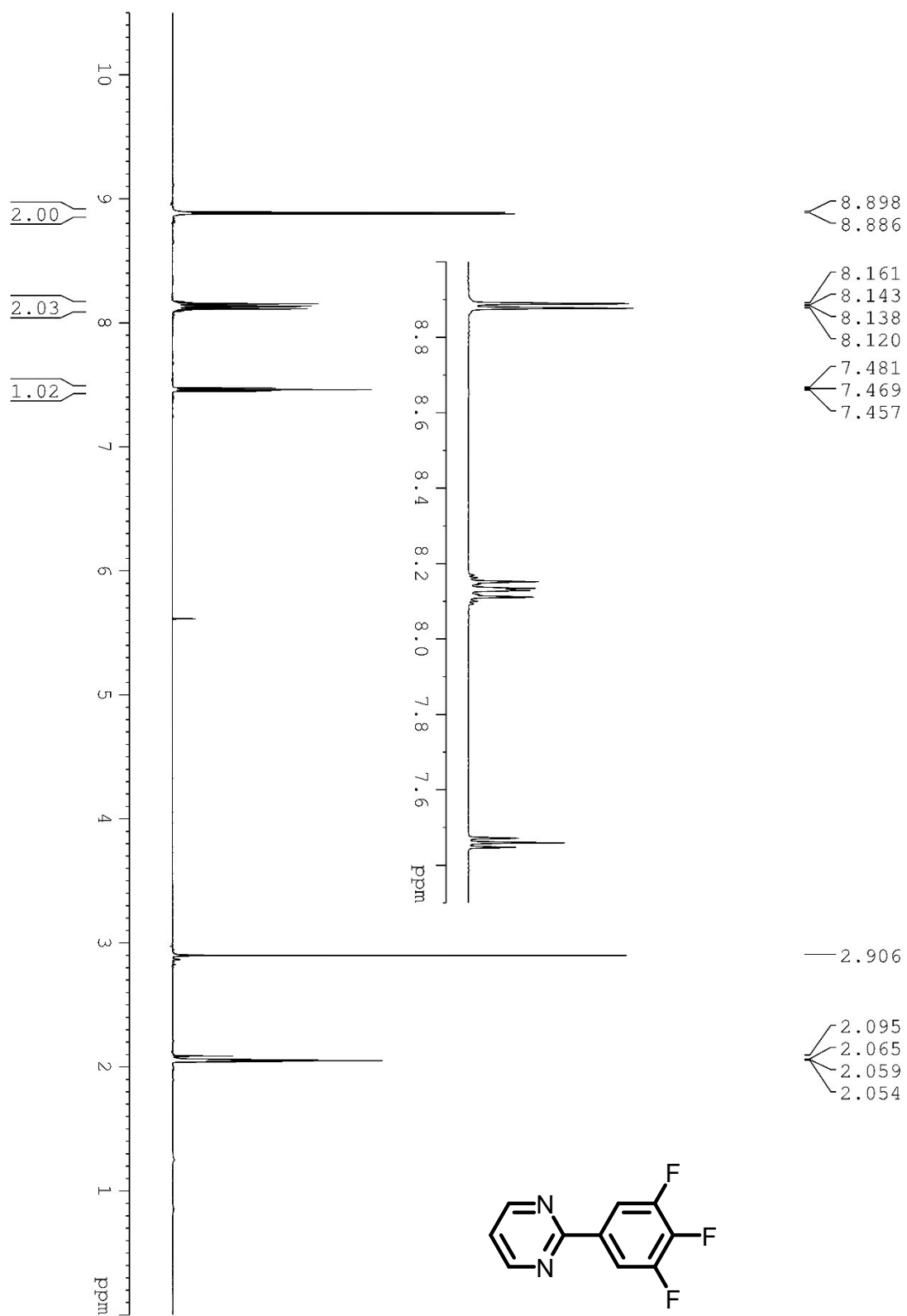


Figure S10. ^{13}C NMR spectrum of compound (2).

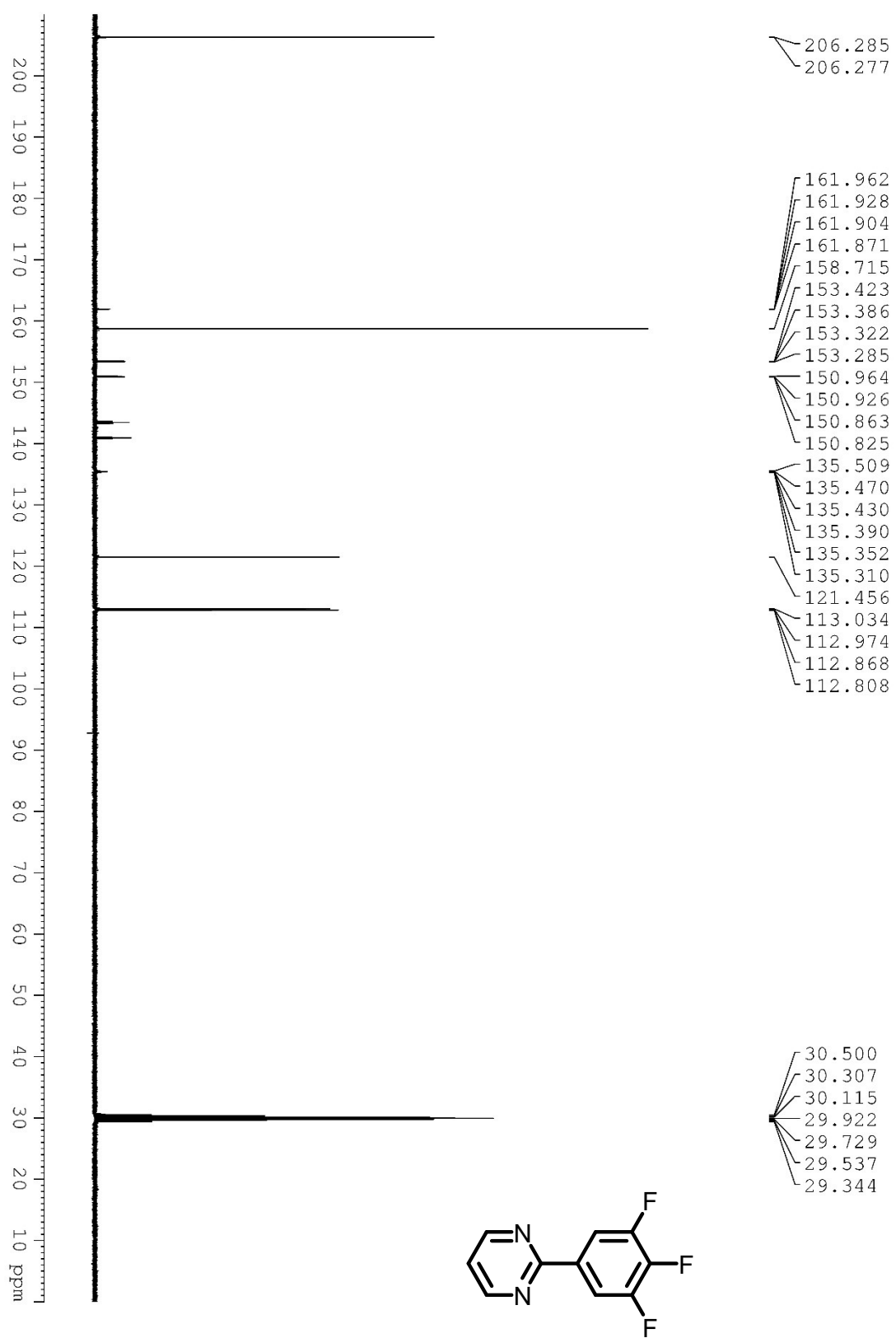
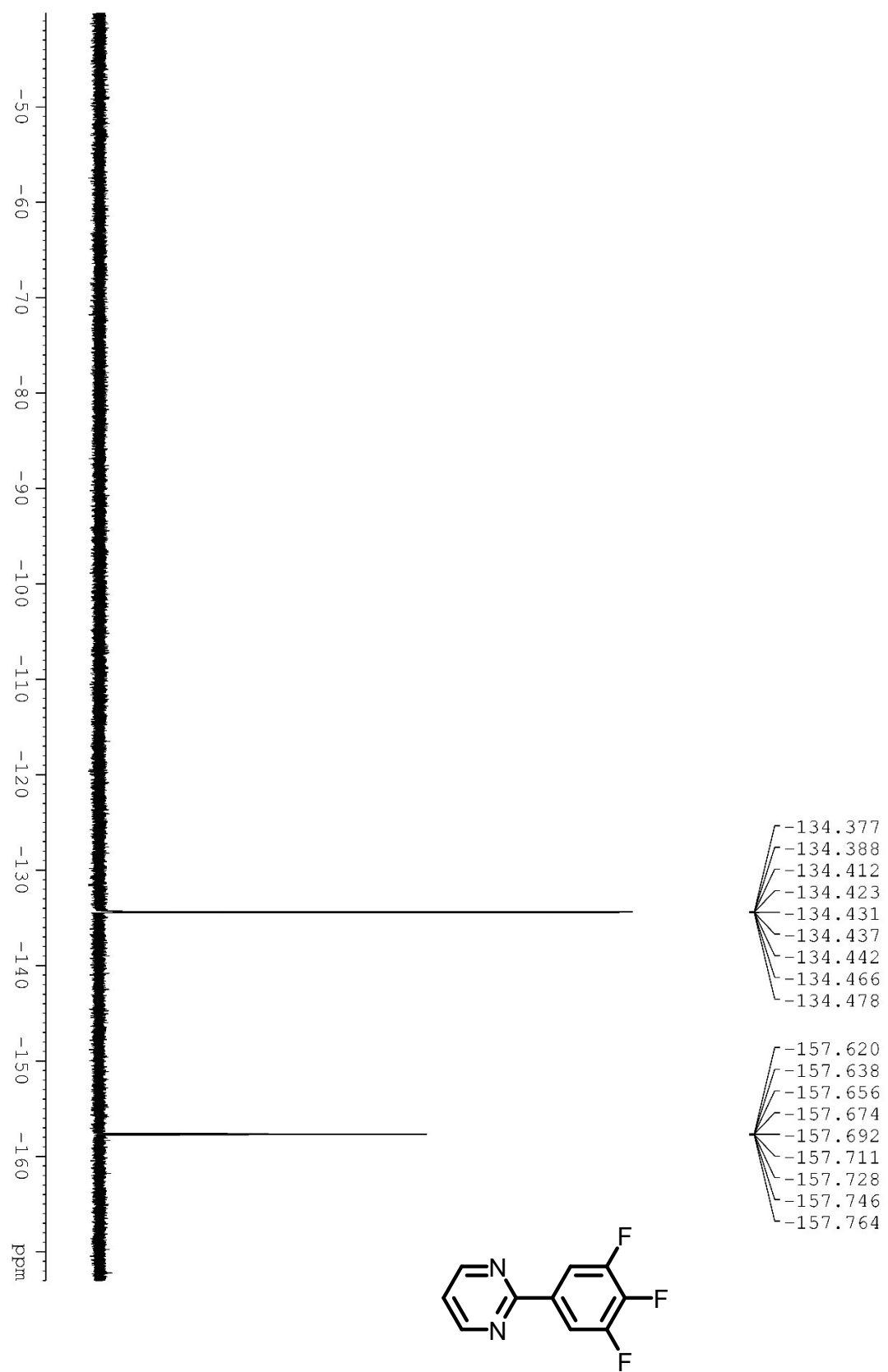
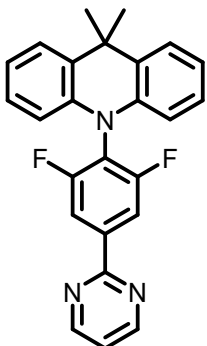


Figure S11. ^{19}F NMR spectrum of compound (2).



10-(2,6-difluoro-4-(pyrimidin-2-yl)phenyl)-9,9-dimethyl-9,10-dihydroacridine (4)



A mixture of compound **2** (0.6221 g, 3 mmol), 9-dimethyl-9,10-dihydroacridine (0.7542 g, 3.0 mmol) and Cs₂CO₃ (1.476 g, 4.5 mmol) were dissolved in DMSO (3 mL) and reacted at 120 °C under argon for 12 hr. After the reaction, the solvent was removed by vacuum distillation. The residue was dissolved in DCM and washed with water and saturated NaCl solution. The organic layer was dried by anhydrous MgSO₄. The crude was further purified through chromatography with Hexanes/ DCM = 1/2 to DCM as eluent to afford purified product **4** as a white solid (0.7902 g, 66 % yield).

¹H NMR (400 MHz, Chloroform-*d*₁): δ 8.86 (d, *J* = 4.8 Hz, 2 H), δ 8.28 (d, *J* = 8.4 Hz, 2 H), δ 7.48 (d, *J* = 7.2 Hz, 2 H), δ 7.29 (t, *J* = 4.8 Hz, 1 H), δ 7.05-6.96 (m, 4 H), δ 6.40 (d, *J* = 7.6 Hz, 2 H), δ 1.69 (s, 6 H); ¹³C NMR (100 MHz, Chloroform-*d*₁): δ 162.16, 161.52 (dd, ¹*J*_{CF} = 253 Hz, ²*J*_{CF} = 5 Hz), 157.50, 140.29, 139.08, 131.00, 126.75, 125.23, 121.60, 120.16, 113.04, 112.69, 112.45, 36.11, 30.58; HRMS calcd. for C₂₅H₂₀F₂N₃ (M+1⁺) 400.1620, obsd. 400.1607

Figure S12. ^1H NMR spectrum of compound (4).

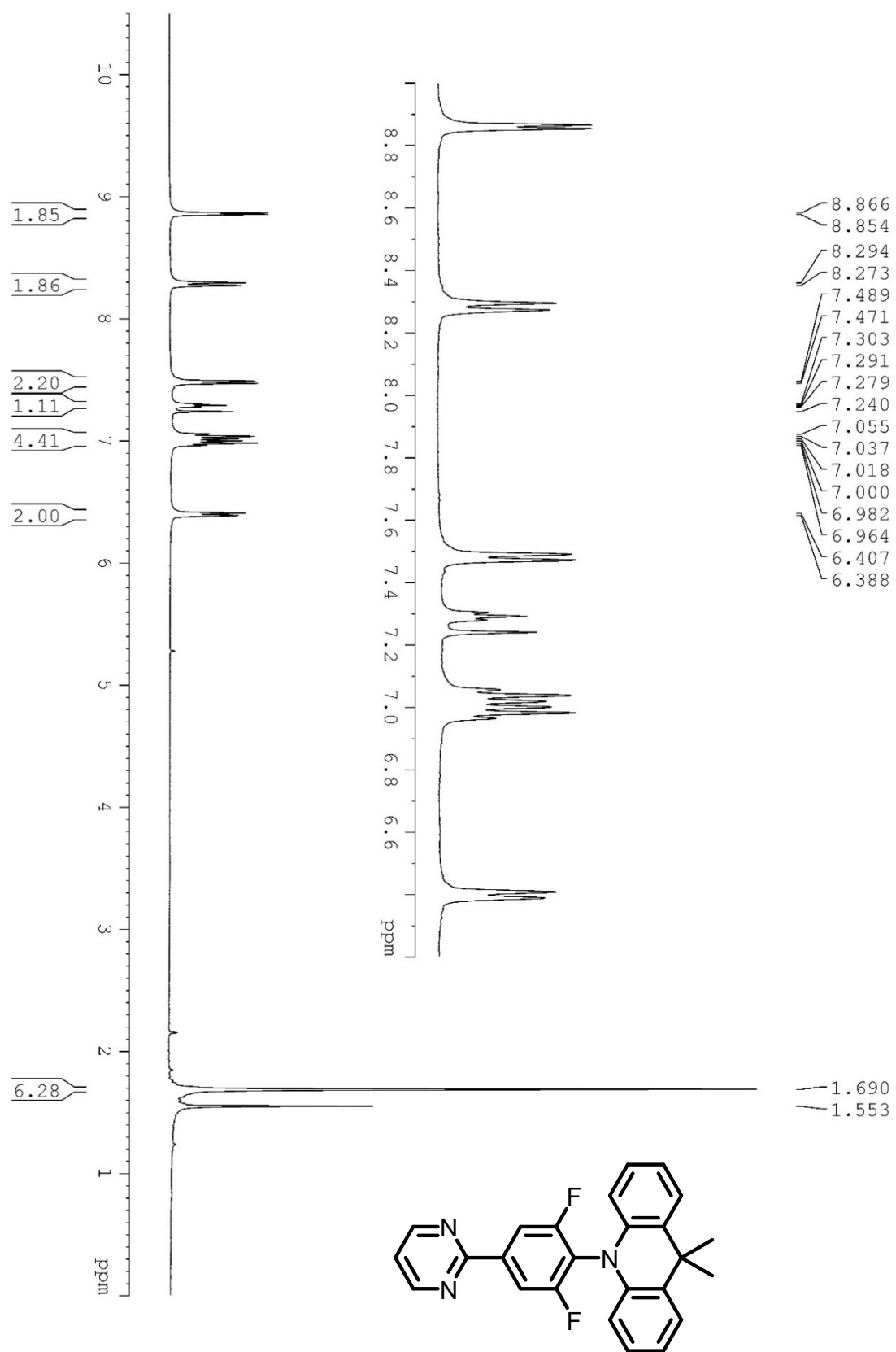


Figure S13. ^{13}C NMR spectrum of compound (4).

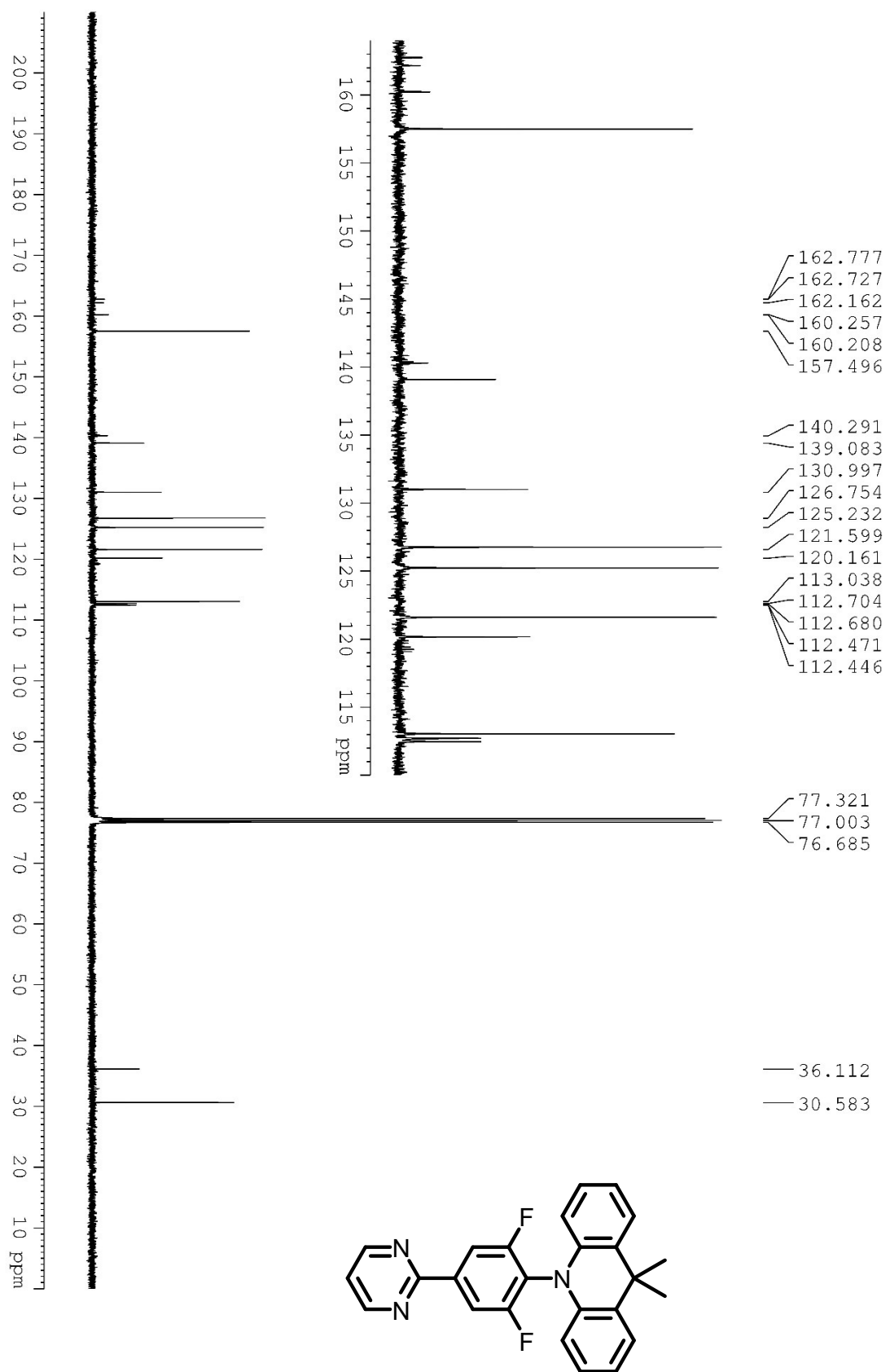
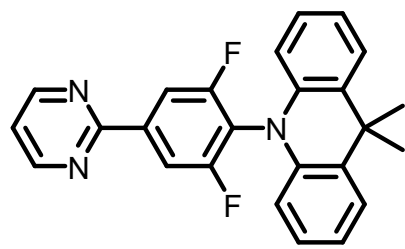
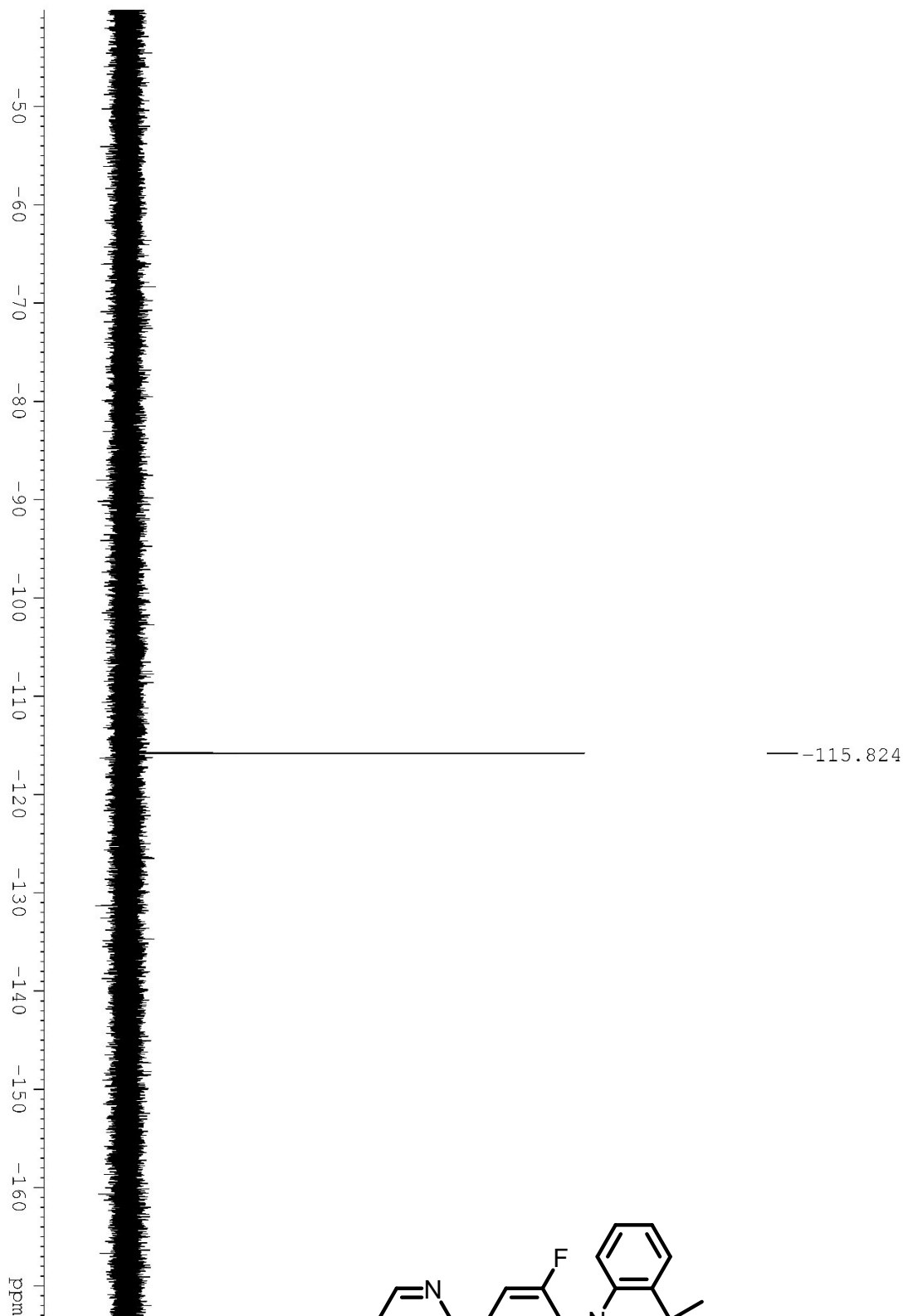
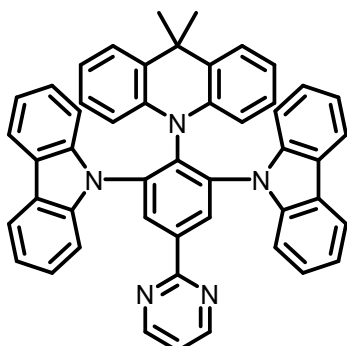


Figure S14. ^{19}F NMR spectrum of compound (4).



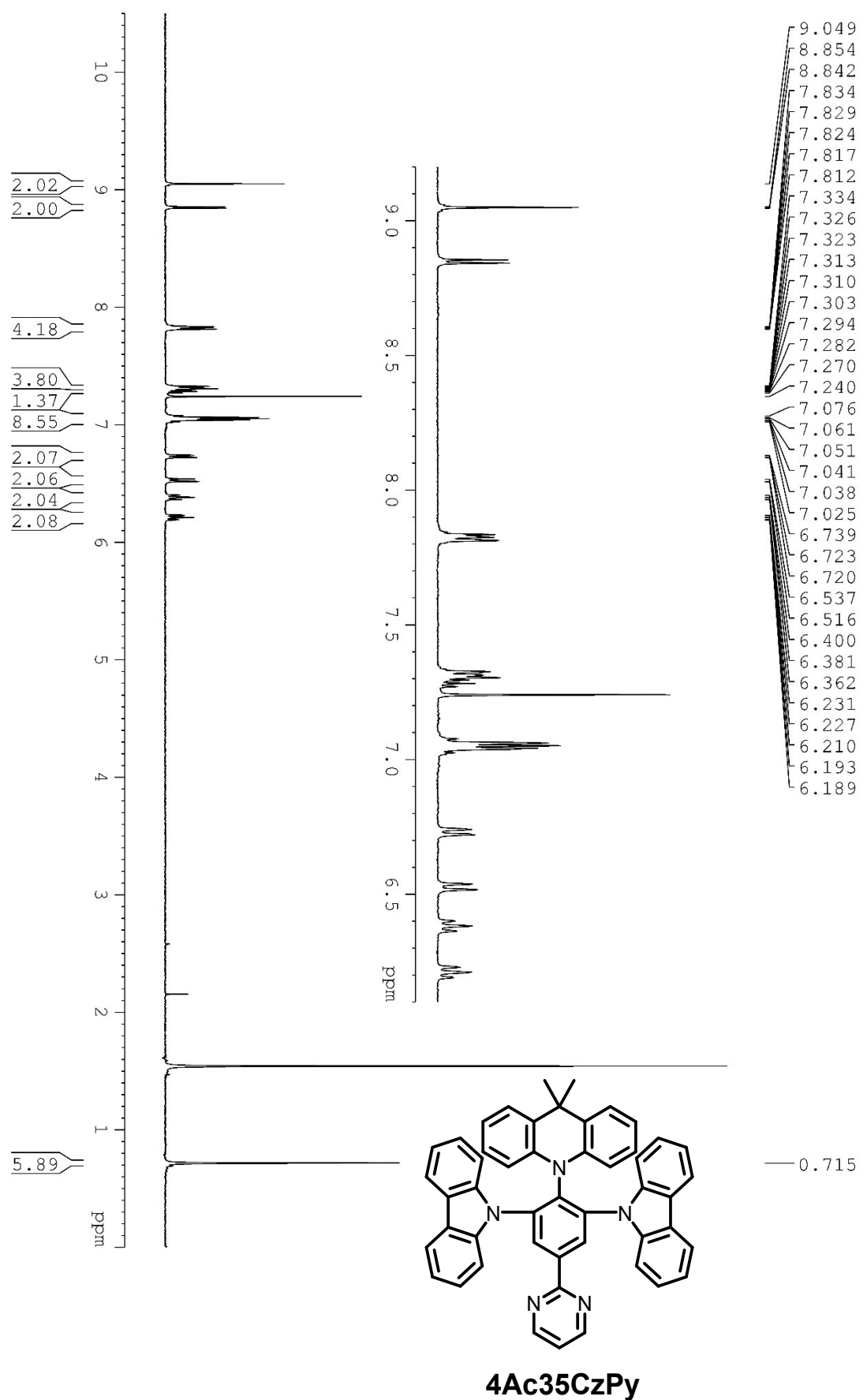
10-(2,6-di(9H-carbazol-9-yl)-4-(pyrimidin-2-yl)phenyl)-9,9-dimethyl-9,10-dihydroacridine (4Ac35CzPy)



A mixture of compound **4** (0.4002 g, 1.0 mmol), carbazole (0.4175 g, 2.5 mmol) and Cs₂CO₃ (0.8247 g, 2.5 mmol) were dissolved in DMSO (1.5 mL) and reacted at 120 °C under argon for 12 hours. After the reaction, the solvent was removed by vacuum distillation. The residue was dissolved in DCM and washed with water and saturated NaCl solution. The organic layer was dried by anhydrous MgSO₄. The crude was further purified through chromatography with Hexanes/ DCM = 1/2 to 1/4 as eluent to afford purified product. The product was further recrystallized in the mixture solution of DCM, acetone, and Hexanes to obtain yellow crystals (0.3540 g, 51 %).

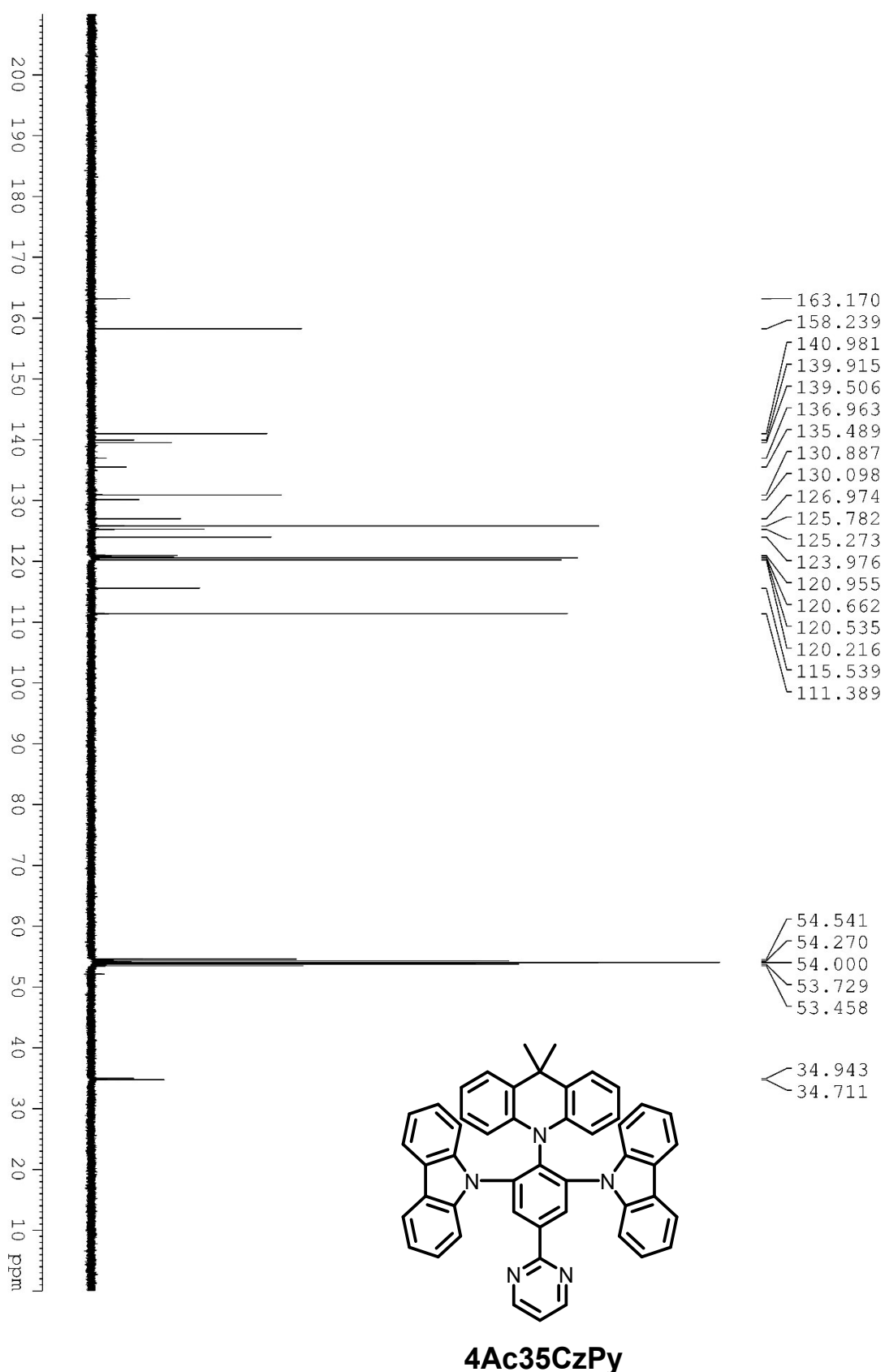
¹H NMR (400 MHz, Chloroform-*d*₁): δ 9.05 (s, 2 H), δ 8.85 (d, *J* = 4.8 Hz, 2 H), δ 7.83-7.81 (m, 4 H), δ 7.33-7.30 (m, 4 H), δ 7.28 (t, *J* = 4.8 Hz, 1 H), δ 7.08-7.02 (m, 9 H), δ 6.73 (d, *J* = 8 Hz, 2 H), δ 6.53 (d, *J* = 8 Hz, 2 H), δ 6.38 (t, *J* = 8 Hz, 2 H), 6.21 (t, *J* = 8 Hz, 2 H), 0.72 (s, 6 H); ¹³C NMR (100 MHz, CD₂Cl₂): δ 163.17, 158.24, 140.98, 139.92, 139.51, 136.96, 135.49, 130.89, 130.10, 126.97, 125.78, 125.27, 123.98, 120.96, 120.66, 120.54, 120.22, 115.54, 111.39, 34.93, 34.71; HRMS calcd. for C₄₉H₃₆N₅ (M+1⁺) 694.2965, obsd. 694.2925; Elemental analysis calcd. for C (84.82%), N (10.09%), H (5.08%), obsd. C (84.850%), N (10.14%), H (4.964%)

Figure S15. ^1H NMR spectrum of 4Ac35CzPy.

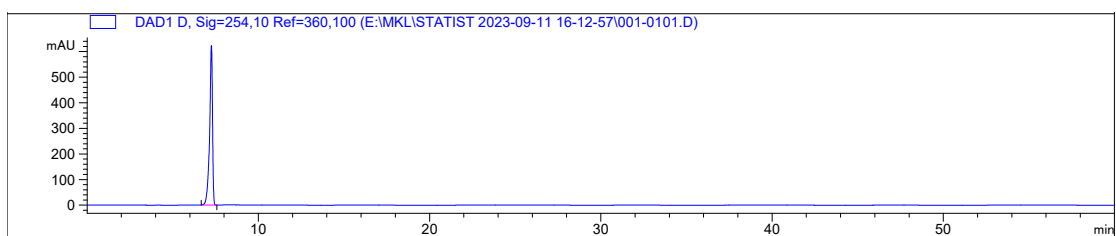


4Ac35CzPy

Figure S16. ^{13}C NMR spectrum of **4Ac35CzPy**.



(a)



(b)

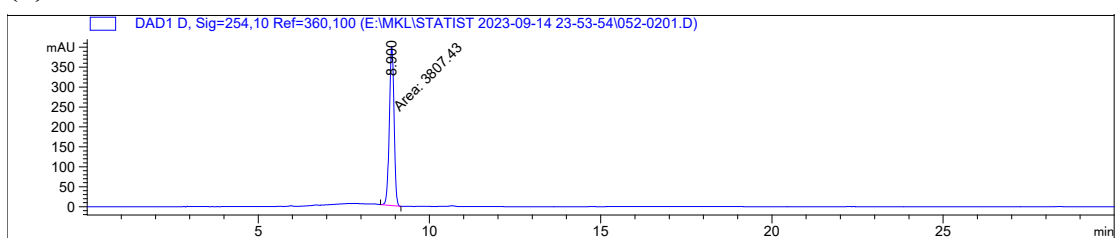
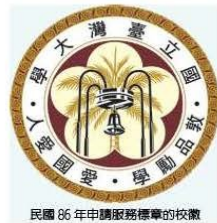


Figure S17. High performance liquid chromatography (HPLC) spectra of (a) **4Ac25CzPy** and (b) **4Ac35CzPy**

國立台灣大學理學院貴重儀器使用中心 元素分析儀報告書

Precision Instrumentation Center—Elemental Analysis Report
College of Science, National Taiwan University



說明： 1.本文件為學術檢測成果，不作認證、法律訴訟及商業廣告使用。

This result is for academic use only, not to be used for any judicial or commercial advertising purpose.

2. Instrument：德國 elementar UNI cube 型 (for NCSH, German)

Accuracy: $\pm 0.1\%$

Precision: $\pm 0.2\%$

Inaccuracy of instrument: $\pm 0.3\%$

3. 儀器負責人：汪根權教授

技術員：陸靖蔚

Instrument Director: Prof. Wong, Ken-Tsung Operator: Ching-Wei Lu

Web. NO. 52023080025

User name 李怡蓁

Supervisor 梁文傑

Department 台大 化學系

Acceptance date 2023/9/1

Analysis date 2023/9/4

Sample code	Date	Time	Weight(mg)	Grp	N%	C%	S%	H%	Repeat	Charge
acetanilide standard 測出值	2023-09-04		4.307	standard	10.360	71.090	0.000	6.710		
	2023-09-04		4.024		10.360	71.050	0.000	6.702		
4AC25CzPy	2023-09-04		4.044		10.090	84.660		4.926	1	
4AC25CzPy	2023-09-04		4.230		10.090	84.630		4.949	1	\$ 240
4AC35CzPy	2023-09-04		4.182		10.140	84.850		4.964	1	
4AC35CzPy	2023-09-04		4.089		10.100	84.690		4.977	1	\$ 240

4 \$ 480

Figure S18. Elemental analysis of 4Ac25CzPy and 4Ac35CzPy

The elemental analysis measurements in this study were conducted by the Precision Instrumentation Center at National Taiwan University.

Table S1. TDA-B3LYP/def2-TZVP(-f)/CPCM(2-MeTHF) vertical excitation energies (in eV) for singlet and triplet excited states of **4Ac25CzPy** and **4Ac35CzPy**. The S_0 minimum structure was used in the calculation of vertical excitation energies.

4Ac25CzPy				4Ac35CzPy			
Singlet States		Triplet States		Singlet States		Triplet States	
S_1	2.853	T_1	2.782	S_1	2.731	T_1	2.561
S_2	3.219	T_2	3.082	S_2	3.192	T_2	3.056
S_3	3.404	T_3	3.320	S_3	3.219	T_3	3.101
S_4	3.413	T_4	3.335	S_4	3.266	T_4	3.199

Calculation of Adiabatic Singlet-Triplet Energy Gap, ΔE_{ST}^{Adia} , Spin-orbit coupling matrix elements, and reorganization energies

The adiabatic singlet-triplet energy gap was calculated by taking the energy difference of the S_1 and T_1 states at their respective minimum geometries.

$$\Delta E_{ST}^{Adia} = E_{S_1}(R_{S1}) - E_{T_1}(R_{T1}),$$

where $E_i(R_j)$ refers to the energy of the i^{th} state at the j^{th} state geometry.

The reorganization energies were calculated as follows:

$$\lambda_S = E_{S_1}(R_{T1}) - E_{S_1}(R_{S1}),$$

$$\lambda_T = E_{T_1}(R_{S1}) - E_{T_1}(R_{T1}).$$

The spin-orbit coupling matrix elements were calculated based on the T_1 state's minimum geometry. From here, the ISC and RISC rates were estimated using the semiclassical Marcus theory.

$$k = \frac{2\pi}{\hbar} V^2 \sqrt{\frac{1}{4\pi k_b T}} \exp\left[-\frac{(\Delta E_{ST}^{Adia} + \lambda)^2}{4k_b T \lambda}\right]$$

Here, the temperature was set to $T=300\text{K}$. In calculating the ISC rate constant, $\lambda = \lambda_T$

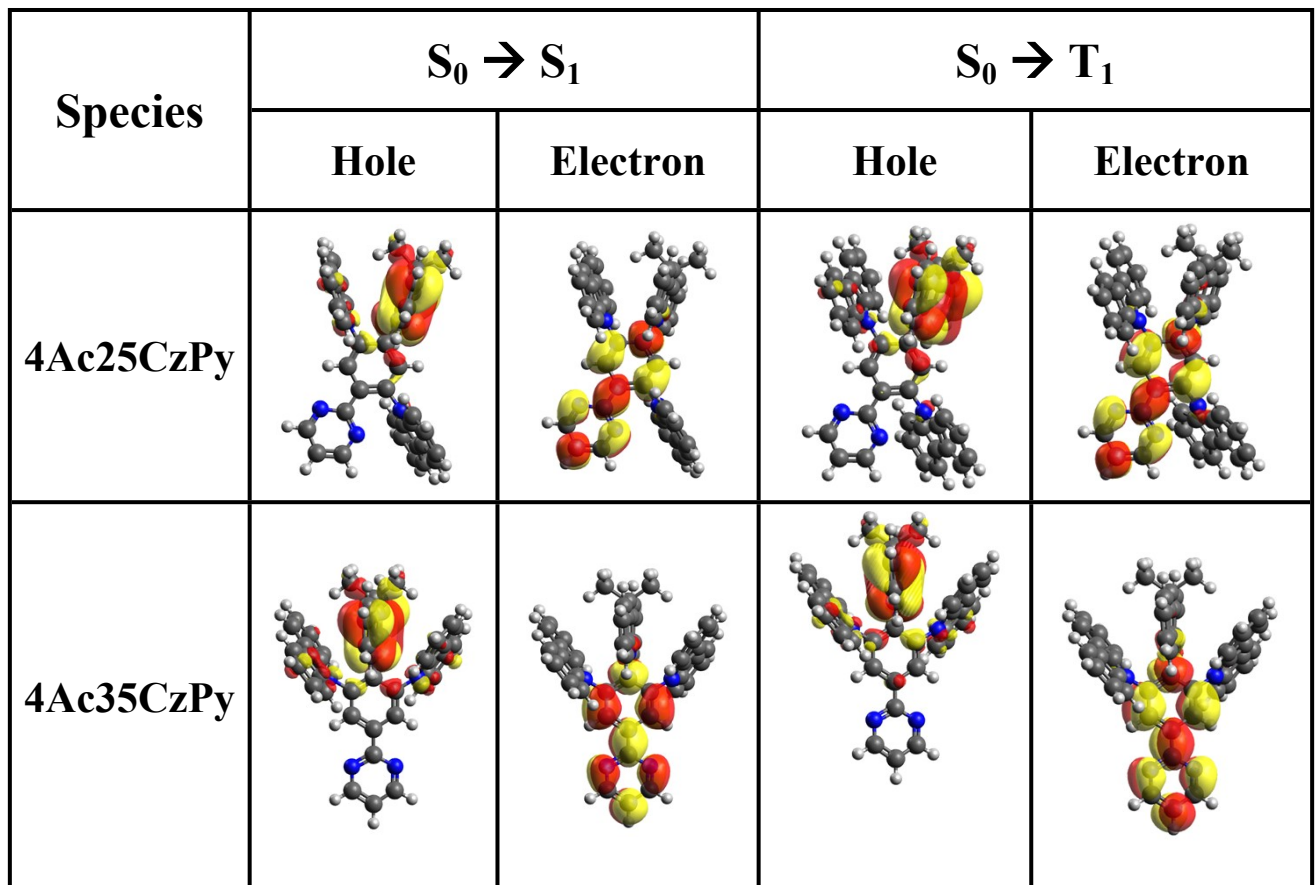
and $\Delta E_{ST}^{Adia} = E_{T_1}(R_{T1}) - E_{S_1}(R_{S1})$. Meanwhile, in calculating the RISC rate constant,

$$\lambda = \lambda_S \text{ and } \Delta E_{ST}^{Adia} = E_{S_1}(R_{S1}) - E_{T_1}(R_{T1}), V^2 = \frac{1}{3} |\langle T_1 | H_{SO} | S_1 \rangle|^2$$

Table S2. Calculated adiabatic singlet-triplet energy gap ΔE_{ST}^{Adia} (eV), spin-orbit coupling matrix elements $|\langle T_1 | H_{SO} | S_1 \rangle|$ (cm^{-1}), reorganization energies λ_S and λ_T (eV), and ISC and RISC rate constants k_{ISC} and k_{RISC} (s^{-1}).

Species	ΔE_{ST}^{Adia} (eV)	$ \langle T_1 H_{SO} S_1 \rangle $ (cm^{-1})	λ_T (eV)	k_{ISC} (s^{-1})	λ_S (eV)	k_{RISC} (s^{-1})
4Ac25CzPy	0.038	0.224	0.0134	2.37×10^7	0.0795	2.82×10^6
4Ac35CzPy	0.088	0.210	0.0241	4.70×10^6	0.0742	4.49×10^5

Table S3. TDA-B3LYP-D3BJ/def2-TZVP(-f)/CPCM(2-MeTHF) natural transition orbital (NTO) analysis for the S_1 and T_1 states of 4Ac25CzPy and 4Ac35CzPy at their minimum respective excited state minimum structures.



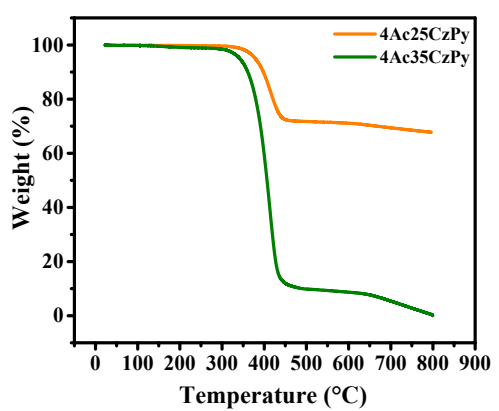
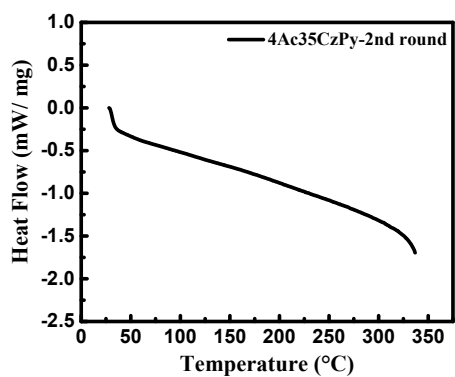
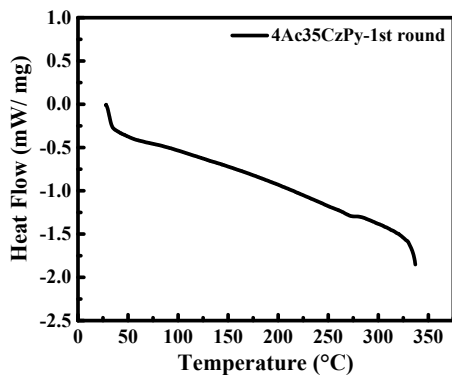


Figure S19. Thermal gravity analysis (TGA) curves of **4Ac25CzPy** and **4Ac35CzPy**

(a)



(b)

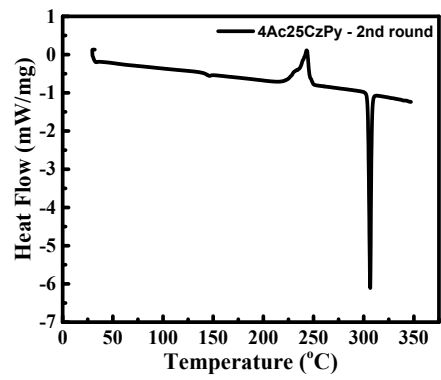
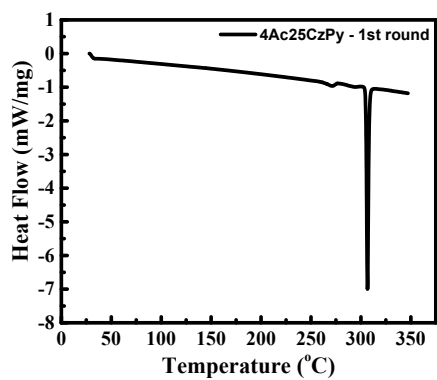
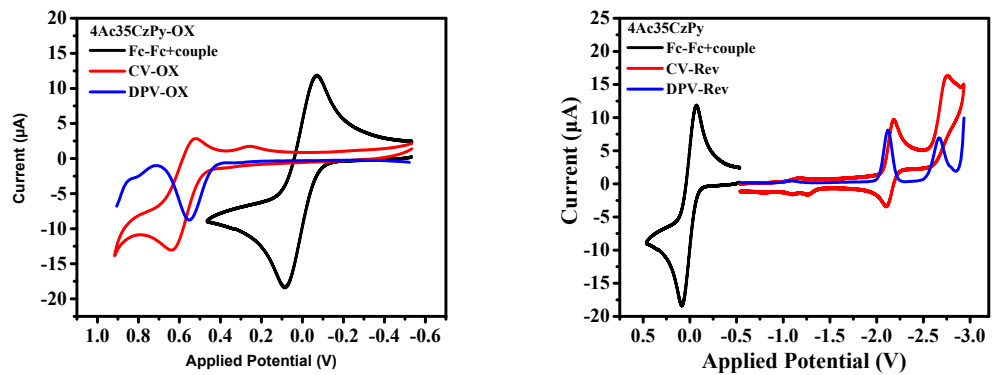


Figure S20. Differential scanning calorimetry (DSC) curves of (a) **4Ac35CzPy** and (b) **4Ac25CzPy**

(a)



(b)

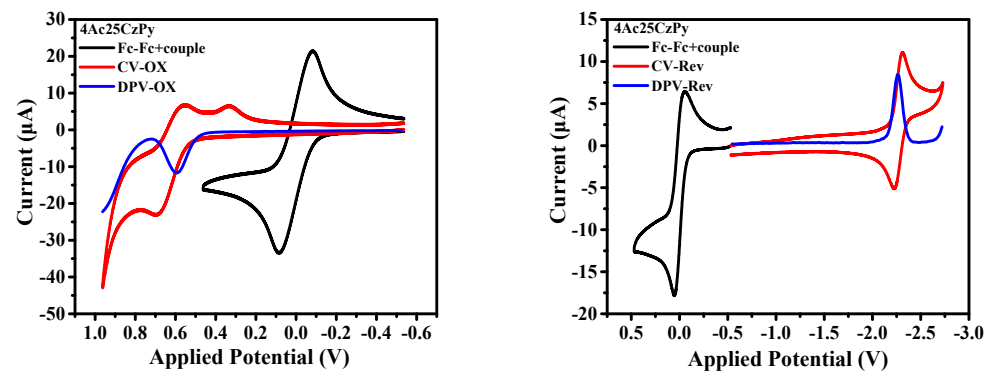


Figure S21. Cyclic voltammogram (CV) and differential pulse voltammetry (DPV) of
(a) 4Ac35CzPy and (b) 4Ac25CzPy

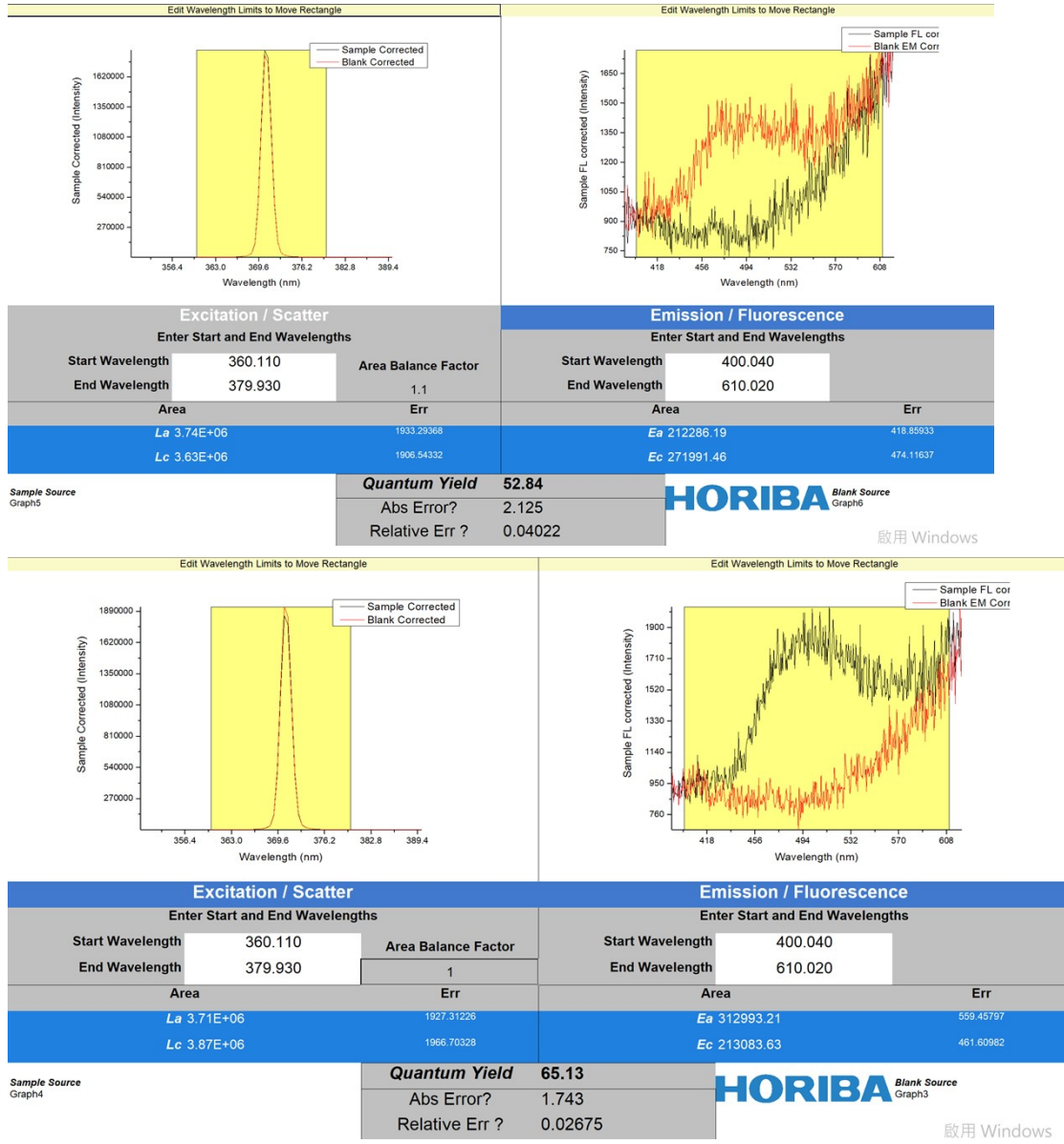


Figure S22. PLQY of mixed film (a) 4Ac25CzPy doped *o*-DiCbzBZ; (b) 4Ac35CzPy doped *o*-DiCbzBZ.

Analysis of rate constant for 4Ac25CzPy and 4Ac35CzPy

With the PL efficiencies ($\Phi_{total}/\Phi_{prompt}/\Phi_{delayed}$) and decay times (τ_p, τ_d) of **4Ac25CzPy** and **4Ac35CzPy**-doped films, we can evaluate the rate constants of **4Ac25CzPy** and **4Ac35CzPy**-doped films via following equations.

$$K_{r,s} = \Phi_{prompt} k_p \quad (1)$$

$$K_{ISC} = (1 - \Phi_{prompt}) k_p \quad (2)$$

$$K_{rISC} = \frac{k_p k_d \Phi_{delayed}}{K_{ISC} \Phi_{prompt}} \quad (3)$$

$$K_{nr,T} = k_d - \Phi_{prompt} K_{rISC} \quad (4)$$

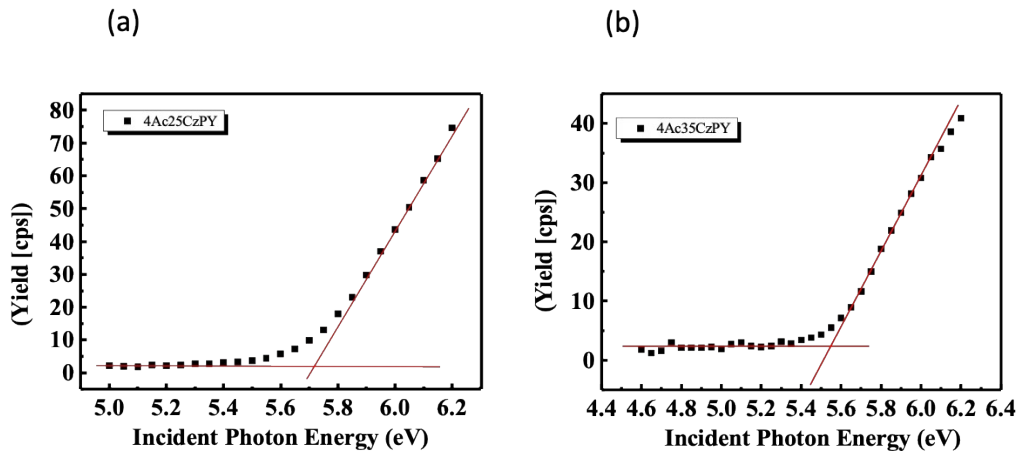


Figure S23. Photoelectron spectra for (a) **4Ac25CzPy** and (b) **4Ac35CzPy** measured by AC-II.

Table S4. Device structure of OLEDs with **4Ac35CzPy** as emitter.

Device	HTL TAPC	EBL <i>mCP</i>	EML o-DiCbzBz/ X% 4Ac35CzPy	ETL DPPS	cathode LiF/Al
3A-5			30 /9%		
3A-2			30 /12%	55	
3A-6			30 /15%		
3A-9				50	
3A-2	50	10	30 /12%	55	0.8/120
3A-10				60	
3A-11				65	
3A-10			25/12%		
3A-2			30/12%	55	
3A-11			35/12%		

unit: nm

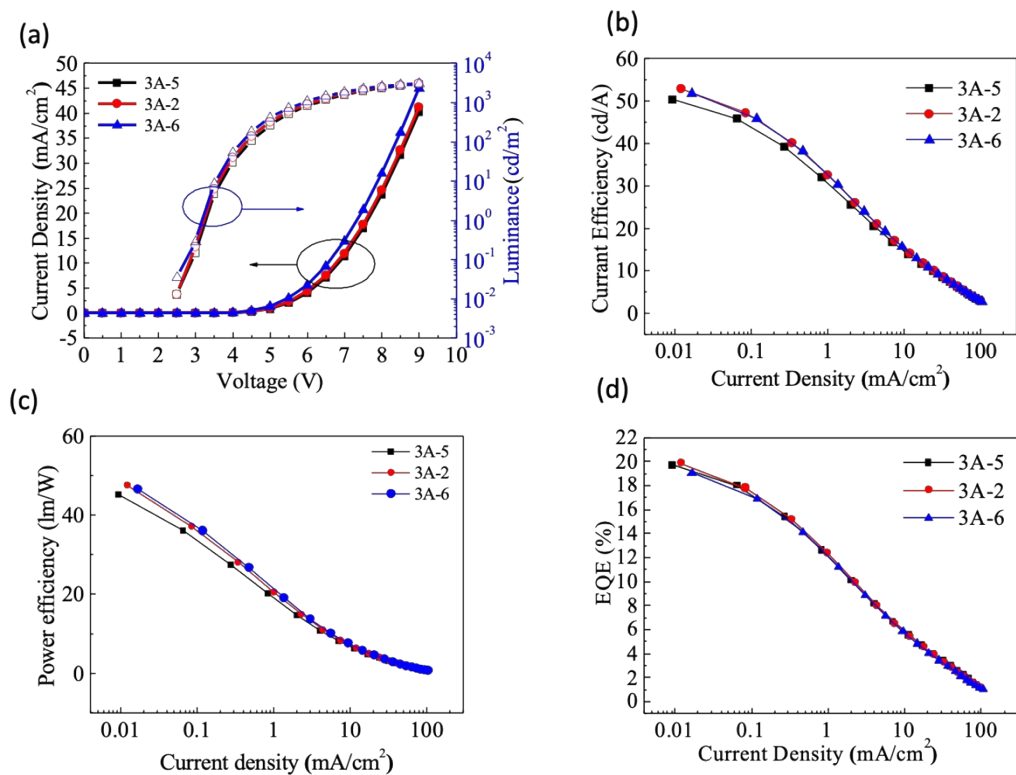


Figure S24. Device performance of (a) J-V; (b)CE-J; (c)PE-J; (d) EQE-J for OLEDs (3A-5, 3A-2, 3A-6).

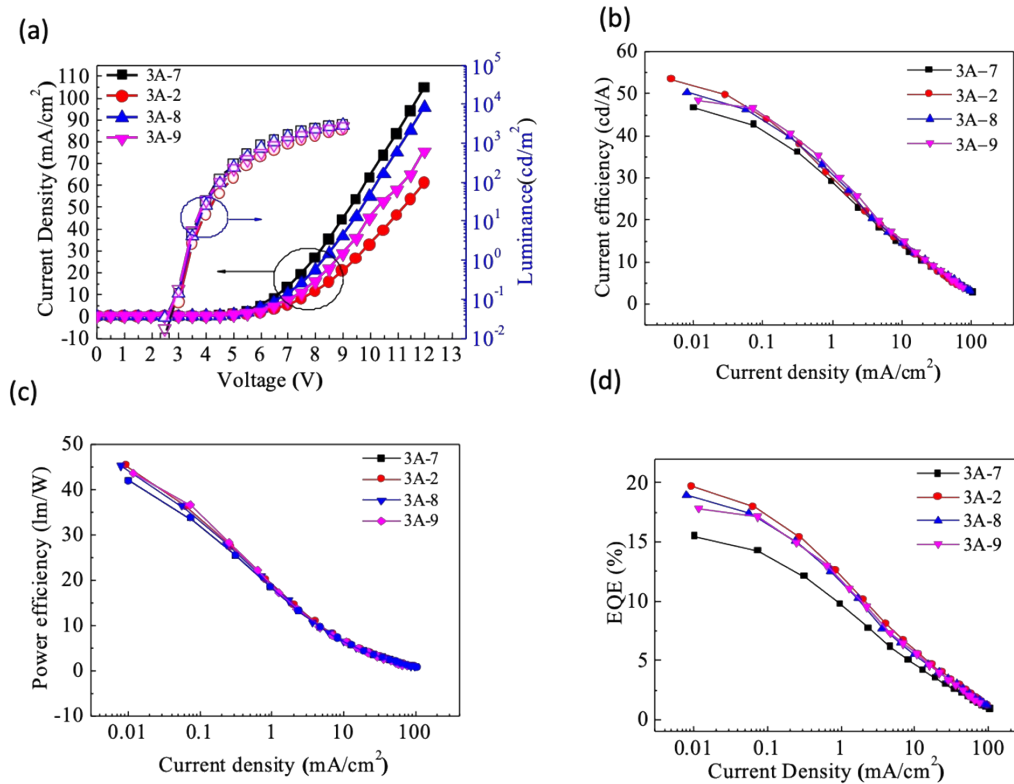


Figure S25. Device performance of (a) J-V; (b)CE-J; (c)PE-J; (d) EQE-J for (3A-7, 3A-2, 3A-8, 3A-9).

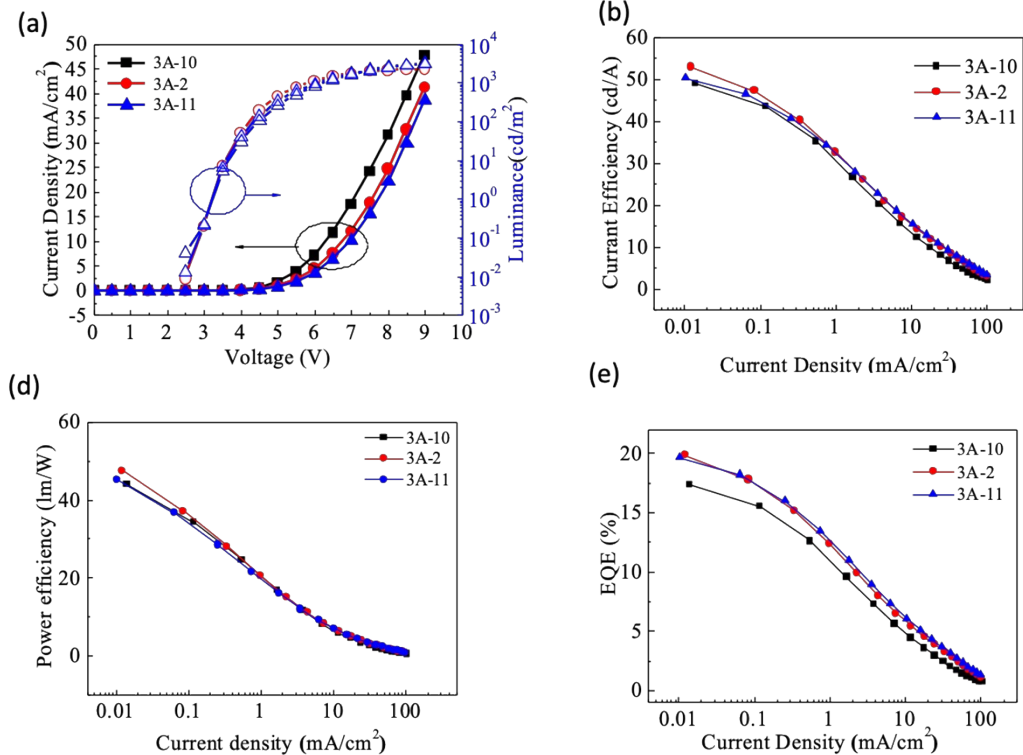


Figure S26. Device performance of (a) J-V; (b)CE-J; (c)PE-J; (d) EQE-J for (3A-10, 3A-2, 3A-11).

Table S5. Device performance for OLEDs with **4Ac35CzPy** as emitter.

Device	EML/ETL (%, nm)	Voltage ^a (V)	Luminance ^b (cd/m ²)	CE ^c (cd/A)	PE ^c (lm/W)	EQE ^c (%)	CIE ^d (x,y)
3A-5	9%, 30 / 55	6.83	3215	50.37/39.65/18.49	45.29/27.92/9.34	19.67/15.53/7.54	(0.178,0.382)
3A-2	12%, 30 / 55	6.76	3288	52.92/42.45/20.18	47.59/30.93/10.35	19.83/15.98/7.63	(0.180,0.395)
3A-6	15%, 30 / 55	6.55	3200	51.88/41.28/20.12	46.66/30.56/10.78	19.02/15.22/7.22	(0.181,0.397)
3A-9	12%, 30 / 50	6.68	3190	46.53/36.83/16.69	41.84/25.26/7.59	15.47/12.33/5.62	(0.173,0.367)
3A-2	12%, 30 / 55	6.76	3215	52.92/42.45/20.18	47.59/30.93/10.35	19.83/15.98/7.63	(0.178,0.382)
3A-10	12%, 30 / 60	6.98	3293	50.27/39.27/18.13	45.21/27.04/8.99	18.92/14.79/6.85	(0.182,0.395)
3A-11	12%, 30 / 65	7.38	3036	48.49/36.89/18.54	43.61/24.07/8.66	17.8/13.58/6.87	(0.186,0.412)
3A-10	12%, 25 / 55	6.29	2271	48.95/39.28/16.94	44.07/25.52/7.66	17.35/14.01/6.11	(0.179,0.386)
3A-2	12%, 30 / 55	6.76	3288	52.92/42.45/20.18	47.59/30.93/10.35	19.83/15.98/7.63	(0.180,0.395)
3A-11	12%, 35 / 55	6.96	3532	50.35/41.25/20.44	45.22/29.05/10.27	19.64/16.16/8.03	(0.179,0.391)

^a at J= 10 mA/cm²; ^b Maximum; ^c CE/PE/EQE measured at maximum/100 cd/m²/1000 cd/m²; ^d at 4 V

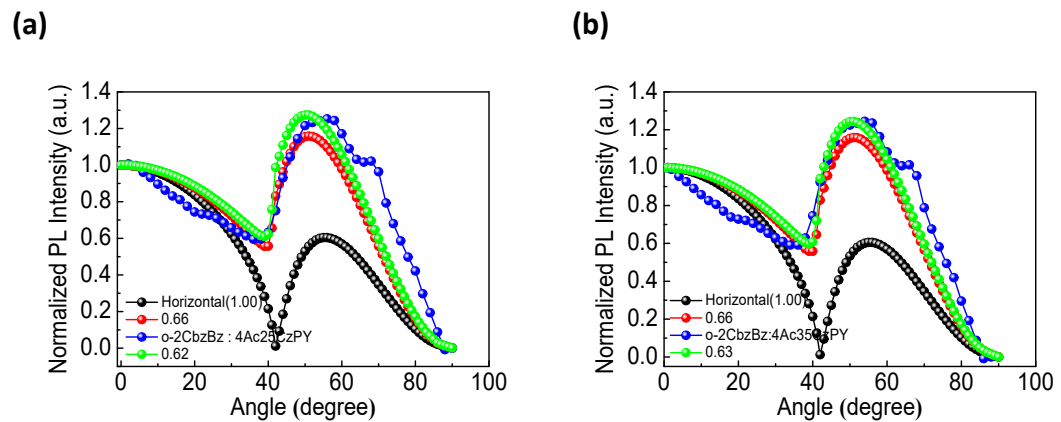


Figure S27. Angle dependent photoluminescence for (a) **4Ac25CzPy** and (b) **4Ac35CzPy**.